Design and applications of MEMS flow sensors

Ejeian, Fatemeh; Azadi, Shohreh; Razmjou, Amir; Orooji, Yasin; Kottapalli, Ajay; Warkiani, Majid Ebrahimi; Asadnia, Mohsen

Published in:
Sensors and Actuators A: Physical

DOI:
10.1016/j.sna.2019.06.020

Publication date:
2019

Sensors and Actuators A 295 (2019) 483–502

Contents lists available at ScienceDirect

Sensors and Actuators A: Physical

journal homepage: www.elsevier.com/locate/sna

Review

Design and applications of MEMS flow sensors: A review

Fatemeh Ejeian[a,b], Shohreh Azadi[a,f], Amir Razmjou[b,c], Yasin Orooji[d], Ajay Kottapalli[e], Majid Ebrahimi Warkiani[f], Mohsen Asadnia[a,*]

[a] School of Engineering, Macquarie University, Sydney, New South Wales, 2109, Australia
[b] Department of Biotechnology, Faculty of Advanced Sciences and Technologies, University of Isfahan, Isfahan, 73441-81746, Iran
[c] UNESCO Centre for Membrane Science and Technology, School of Chemical Engineering, University of New South Wales, Sydney, 2052, Australia
[d] College of Materials Science and Engineering, Nanjing Forestry University, No. 158, Longpan Road, Nanjing, 210037, Jiangsu, People's Republic of China
[e] Department of Advanced production engineering, Engineering and technology institute Groningen, University of Groningen, 9747AG, Groningen, the Netherlands
[f] School of Biomedical Engineering, University of Technology Sydney, Sydney, 2007, Australia

ARTICLE INFO

Article history:
Received 11 February 2019
Received in revised form 10 June 2019
Accepted 11 June 2019
Available online 13 June 2019

Keywords:
Flow sensors
Bio-inspired sensing
Artificial hair cell
Piezoelectric
Piezoresistive
Hot-wire

ABSTRACT

There is an indispensable need for fluid flow rate and direction sensors in various medical, industrial and environmental applications. Besides the critical demands on sensing range of flow parameters (such as rate, velocity, direction and temperature), the properties of different target gases or liquids to be sensed pose challenges to the development of reliable, inexpensive and low powered sensors. This paper presents an overview of the work done on design and development of Microelectromechanical system (MEMS)-based flow sensors in recent years. In spite of using some similar principles, diverse production methods, analysis strategies, and different sensing materials, MEMS flow sensors can be broadly categorized into three main types, namely thermal sensors, piezoresistive sensors and piezoelectric sensors. Additionally, some key challenges and future prospects for the use of the MEMS flow sensors are discussed briefly.

Contents

* Corresponding author.
E-mail address: mohsen.asadnia@mq.edu.au (M. Asadnia).

https://doi.org/10.1016/j.sna.2019.06.020
0924-4247/

1. Introduction

Flow sensors are required to measure the rate and direction of liquid and gas flows in various applications, including determination of flow patterns [1], measurement of wall shear stress [2], viscosity [3], and density measurements [4]. During the past decades, numerous types of sensing devices have been developed and become commercially available for flow measurement [5,6]. It is understood that the flow as measured may be influenced by velocity, pressure, temperature or chemical content of the systems [7]. Therefore, flow sensing devices are typically based on the direct detection of volume, mass, velocity, or combination thereof, by measuring a variety of physical variables [8,9].

Over the past few decades, microelectromechanical system (MEMS) technology has opened up new avenues in developing flow sensors for various applications. MEMS devices were firstly proposed in the 1960's, following the investigation of the piezoresistive potential of silicon and germanium. The research and development in this field have progressively scaled up since the 1980s [10]. MEMS devices offer characteristics such as small size, low-cost and scalable devices that were not achievable using traditional engineering methods. Recently, microfabrication technologies have been widely employed to fabricate MEMS sensors for use in a wide range of applications such as healthcare, physical activities, safety and environmental sensing [11,12]. MEMS flow sensors miniaturised devices that can achieve high resolution (up to a few micro to nanolitre per minute), and offer a low-cost alternative compared to the traditional sensing devices [13,14]. Due to these fundamental advantages, MEMS flow sensors are used extensively in various applications such as navigation and object detection on autonomous underwater vehicles (AUV) [15,16], flow measurement in biomedical surgery, diagnostic devices, chemistry and therapeutic areas [17], liquid dispensing systems [8,18], and gas monitoring systems [19,20].

MEMS flow sensors have been developed in the past using both silicon and polymer materials, and by applying various sensing elements and structural designs. The most common sensing methods are thermal [21,22], torque [23,24] and drag force based [25] flow sensing. Also, MEMS hot wire anemometer sensors have been widely used for air and water flow sensing applications [26,27]. In addition, with the advances in micromachining technology using polymers and non-silicon materials, it has become possible to mimic the stimulus transmission mechanisms of biological sensing systems, such as hair cells and the lateral-line of blind cave fish [28], leaf veins [29], seal whiskers [30], and human hairy skin structure [31] in order to develop miniaturised yet sensitive fluid flow sensors.

In this paper, we provide a comprehensive review of the various micro/nano-scale flow sensors developed to date which falls primarily into three broad categories, depending on the sensing principle employed. The categories are: thermal flow sensors, piezoresistive flow sensors, and piezoelectric flow sensors. We have discussed each of these sensing principles based on the sensing element material for the device. The sensitivity of the sensors has been progressively improved over time by the use of different sensing principles and new sensor structures that enhance the interaction between the sensor and the surrounding fluid. Finally, in section 5, we discuss the challenges, and possible solutions and future perspective of MEMS flow sensors as the next generation sensing device.

2. MEMS thermal flow sensors

Thermal flow sensors utilize the heat transfer intensity in order to determine the flow velocity. This principle provides high sensitivity and accuracy in measurement with low output signal drift. In addition, such sensors feature the advantage of being able to sense without the need for any mechanically moving micro-components [18]. In general, thermal flow sensors consist of two basic parts, namely heaters and sensing elements (Fig. 1.A). A sensing element detects the variation in heat transfer between the heater and the working flow, therefore, the sensitivity of the device improves when more heat is transferred to the working fluid. It appears that one of the most important limitations on accuracy applying to the conventional temperature-based flow sensors is maintaining the temperature on the sensing element accurately [32]. Another challenge associated with thermal flow sensors is their inability to measurement low flow velocities [33]. Sensing elements in traditional hot-wire and hot-film sensors have a high specific heat capacity making it hard to follow the weak heat convection transfer resulting a poor frequency response.

In view of the different methods of heater control and various evaluation modes, three types of thermal flow sensors have been characterised in the past. The first type is hot–wire and hot-film (H-type) sensors which measure the flow by either change of heating power with constant temperature or change of temperature with constant heating power. The difference between them is due to structural design: in hot-wire sensors, the metallic wire resistor is free from the substrate and placed within the flow, whereas in hot-film sensors the resistor is deposited on a membrane placed adjacent to the flow. The second type is calorimetric (C-type) sensors, which evaluate the flow through assessment of changes in heat profile around the heater. The third type is time-of-flight sensors, which assess the flow using the detection of heat pulses in a defined distance from the heater. In this section, the two MEMS thermal flow sensors are detailed.

2.1. Hot–wire/film MEMS thermal flow sensors

Both hot-wire and hot-film flow sensing systems use heated resistive elements in the form of wire or thin film. Their common operating principle is measuring the heat loss in elements due to thermal convection generated by the ambient fluid, that loss having a direct relationship with the flow rate [34]. In order to provide a reasonable sensitivity in various thermal conditions, heat-sensing elements should have a high-temperature coefficient of resistance (TCR). Therefore, MEMS thermal flow sensors are typically composed of silicon or metallic based materials [34] (Table 1).

2.1.1. Silicon-based hot-wire/film MEMS thermal flow sensors

Silicon flow sensors are highly attended in development of MEMS devices, because of their simple and efficient thermal and

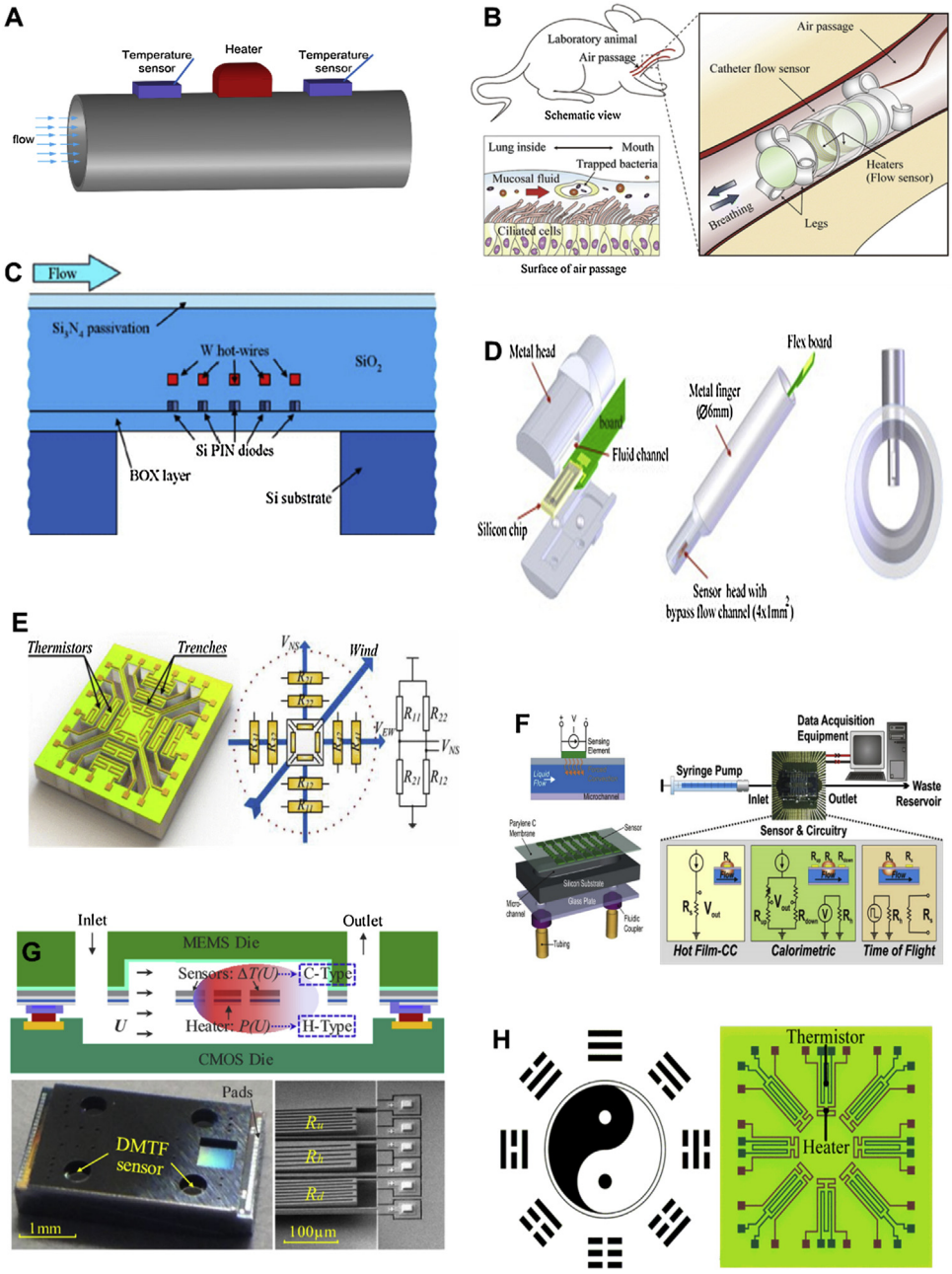

Fig. 1. MEMS thermal flow sensors. (A) The components of a basic thermal mass flow meter including two temperature sensors (upstream and downstream) and a heater. (B) Perspective view of an implantable catheter flow sensor with the ability to anchor onto the inside of the animal's bronchus via its legs [56]. (C) Schematic cross-section view (not to scale) of a thermoelectronic airflow sensor [60]. (D) Schematic view of a calorimetric airflow sensor chip integrated with a metal finger head placed in a tube [92]. (E) Schematic showing an equivalent circuit of a silicon-based thermal wind sensor composed of eight symmetric thermoresistors arranged in two Wheatstone full-bridges [94]. (F) Schematic presentation of a sensing array mechanism, 3-D structure and experimental design of three- mode biocompatible liquid sensing system based on parylene membrane [78]. (G) Schematic drawing and photography of Dual-mode micro thermal flow (DMTF) with the sensing potential in both hot-film and calorimetric mode [71]. (H) Schematic view of an octagonal Eight-Trigrams symbol and the layout of a MEMS thermal wind sensor inspired by this structure [107].

electrical properties. Indeed, poly silicone-based heat elements can be adjusted due to the proper demand by using different type and concentration of dopant [35,36]. An initial study in this field was conducted by Van Oudheusden et al. who described the development of a two-dimensional thermal flow sensor consisting of a thermally isolated floating membrane. This could be considered the first generation of micromachined thermal flow sensors [37]. With four suspension beams, the developed sensors allow measurement of flow for a full range of 360° and sensitivity of 5 $mV\,K^{-1}$. In a later work, Moser et al. aimed to enhance the sensitivity of conventional bipolar type thermopiles by developing silicon-based gas flow sensors utilizing industrial complementary metal-oxide-semiconductor (CMOS) technology [38]. Yoon et al. developed a MEMS-based thermal flow sensor, where an integrated mass flow sensor with on-chip CMOS circuits was paired with a gas type sensor [39]. This sensor was able to measure the gas type, flow velocity, direction, temperature, and pressure. In another effort, Kaltsas et al. presented a CMOS compatible silicon flow sensor with porous silicon for thermal isolation [40]. The device consisted of two thermopiles made up of two series of aluminium/p-type polysilicon thermocouples, which provided a sensitivity of 6.0 $mV/(m/s)W$. Iderj et al. [41] developed a device by mounting two dual MEMS

Table 1
Hot-wire/film MEMS thermal sensors for detection of fluid flow rate and flow direction.

Sensing element material	Configuration	Fluid type	Detection range	Sensitivity	Ref
Si thermopile Pt electrode	Hot-film	Air	12–63 m/s	NA	[37]
3C-SiC thin film heater Ni electrode	Hot-film	Air	0–9 m/s	0.091 1/(m/s)	[19]
Polysilicon resistor	Hot-film	Air	10–30 m/s	NA	[21]
polycrystalline silicon resistor	Hot-film	Air	0–30 m/s	NA	[41]
Pt sensor	Hot-wire	Air	1.5–11 m/s	CV mode0.1433×10^{-4} A$(m/s)^{-1/2}$ CC mode 7.98×10^{-3} V$(m/s)^{-1/2}$	[61]
Pt/Ni/Pt thermal element Cr/Au electrical lead	Hot-wire	Air	0–20 m/s	NA	[62]
Pt thermal element	Hot-wire	Air	0–20 m/s	NA	[63]
Pt thermal element	Hot-wire	Air	13–16.5 m/s	NA	[64]
Pt nanowire	Hot-wire	Air	5–45 m/s	NA	[50]
Au/Cr heater	Hot-wire	Air	0–42.46 m/s	NA	[54,55]
Ni/Pt/Ni/Pt/Ni thermistor Au/Ti heater element	Hot-wire/film	Air	10–40 m/s	NA	[2]
Au/Cr heater	Hot-wire	Air	0–6.37 m/s	NA	[65]
Au/Cr heater	Hot-wire	Air	0–0.11 m/s	NA	[56]
Ti/Pt sensing element	Hot-film	Air	0.1–10 m/s	NA	[66]
Al/Si bond wire	Hot-wire	Air	0.01–17.5 m/s	LF mode: 1.61 V/(m/s) HF mode: 0.586 V/(m/s)	[51]
Pt bond wire	Hot-wire	Air	0.01–17.5 m/s	LF mode: 1.11 V/(m/s) HF mode: 0.196 V/(m/s)	
Ti/Pt/Au & Ti/Cu/Au resistor	Hot-wire	Air	2.5–10 m/s	NA	[67]
Ni/Pt resistor Au heater	Hot-wire/film	Air	0–40 m/s	NA	[68]
Cr/Pt sensing element	Hot-wire	Air	NA	NA	[58,59]
Pt resistor Al lead element	Hot-film	Air	5–15 m/s	NA	[57]
W heater Diode sensing elements	Hot-wire	Air	NA	NA	[60]
Au/Cr heater	Hot-wire	Air	0–0.11 m/s	NA	[69,70]
Polysilicon heater Diode sensing elements	Hot-film	Oil and Air	0–0.8 m/s	NA	[45]
Polysilicon micro heater	Hot-wire/film	Gas, N2	0–73 m/s	NA	[71]
SiO_2-Si_3N_4/SiN_x membrane	Hot-wire	Natural gases	0–6 m^3/h	NA	[72]
Pt thermistors	Anemometric Calorimetric	Gas	0.05–10 m/s	NA	[73]
Cu line resistors	Hot-wire	Carrier gas	NA	NA	[74]
Polysilicon heater Au/Cr detector	Hot-film	Gas	0.01–5 m/s	6.8×10^{-3} 1/(m/s)	[39]
Al/polysilicon thermocouples Polysilicon heater	Hot-film	Gas, N_2	0–0.4 m/s	6×10^{-3} V/(m/s)W	[40]
Ni resistors	Hot-film	Different gas mixtures	0–5 m/s	2.6×10^{-2} V/(m/s)	[47]
Au heater	Hot-film	Gas, N_2 DI water	0.34–34.72 m/s 0.5–0.028 m/s	NA	[75]
B-doped Polysilicon heater	Hot-film	DI water	0–8.25×10^{-3} m/s	0.87 V/(m/s)	[42]
polycrystalline Si resistor	Hot-film	Water	0–30.96 m/s	NA	[18]
Pt sensing element	Hot-film	DI water	0–0.01 m/s	0.153 V/(m/s)	[76]
Ni/Pt thermal element	Hot-wire	Water	NA	NA	[48]
Ni/Fe thermal element	Hot-wire	Water	0–0.25 m/s	NA	[77]
W/Ti/Pt thermal element	Hot-film Time-of-flight	DI water	0–0.013 m/s	2.14×10^{-6} V/(m/s)	[78]
Pt resistive	Hot-wire	Water	10^{-6}–10 m/s	NA	[79]
Pt heater Cr thermocouple	Hot-film	Blood	0–2.2×10^{-3} m/s	NA	[80]

Al, Aluminum; Au, Gold; B, Boron; CC, Constant-current mode; CV, Constant-voltage mode; Cr, Chromium; Cu, Copper; DI water, Deionized water; HF, High flow (>2 m/s); LF, Low flow (<0.5 m/s); NA, Not available data; Ni, Nickle; ; Pt, Platinum; Re. No: Reynolds numbers; Si, Silicon; SiO_2, Silicon dioxide; Si_3N_4, Silicon nitride; Ti, Titanium; W, Tungsten.

hot-film sensor chips on a cylindrical probe, where each chip was embedded in to a concave surface to minimise the thermal interaction between the two sensitive elements. They showed the sensor performance of the device in the range 0 to 30 m/s (speed) and 5.6×10^{-4} ° RMS (root mean square error) (direction). The power consumption of the device is 80 mW. Wu and co-workers developed a MEMS thermal flow sensor that measured liquid flow rate in the range of nanolitre per minute [42]. The sensor consisted of a polysilicon thin-film heater that was placed on the wall of a microchannel fabricated on a silicon substrate. The sensor operated on the principle of convective heat transfer from the heater to the liquid flow in the microchannel, in which the liquid flow rate was measured by detecting the change of temperature. This device reached the highest temperature to flow ratio of $0.026\,^{\circ}/nl\,min^{-1}$, by using a relatively long boron-doped polysilicon thin film in a suspended microchannel, which effectively improved the sensitivity of flow velocity measurement.

In the case of thermoelectric flow sensors, the presence of a diode/transistor provides an excellent platform to locate the sensor in the hottest zone of the heating element, which dramatically improves the sensitivity of the device [34]. However, due to some serious drawbacks such as high power consumption and low heat flux, only limited studies have been focused on applying this method [43–45]. By contrast, thermoresistive sensors have been

widely used in thermal sensing mechanisms. As a novel approach, a thin film of silicon carbide (SiC) on a Si substrate formed a highly sensitive, economical and simple thermal flow sensor [19]. In this study, the direct growth of a single crystalline layer of 3C-SiC was followed by patterning of a nickel electrode structure; hence, the effect of different geometrical futures of heater was also analyzed.

2.1.2. Metallic-based hot-wire/film MEMS thermal flow sensors

In general, metals present a positive TCR in the range of 4000 to 7000 ppm/K; However, based on their temperature to electrical resistance ratio, metallic-based heat sensing elements are normally composed of platinum, nickel, copper and gold [46]. As a preliminary work in this field, Qiu and colleagues [47] developed a micro flow sensor with an integrated heat sink and flow guide on the backside of the micro sensor. The heat sink and flow guide were constructed from a thin electroplated gold layer. In another study, Pandya et al. developed a biomimetic artificial lateral line system of MEMS hot-wire anemometer flow sensors [48,49]. The sensing principle of this sensor relied on convection cooling of an initially heated metallic hot–wire element when it was exposed to a flow medium as the heat was transferred from the element to the fluid hence, causing a resistance change. In this study, a model was developed for the MEMS hot-wire anemometers by using a Gaussian mixture model. The training approach produced more accurate results via the measurement results, and can be implemented on static and real-time systems directly. However, this approach was cumbersome to fabricate and more costly more for a system-level implementation. In [50], a 100 nm × 2 μm × 60 μm wire is fabricated to improve the device performance and measure the frequency response. However, the length of the hot-wire is relatively small, leading to a quantity of heat loss at the edge of the wire, restricting the sensitivity and accuracy of the sensor. Bonding hair-like hot-wire structures on the substrate by utilizing integrated circuit (IC) packaging technique formed cheap and easy processing anemometers with a higher area for air flow detection [51]. This instrument composed of a variety of wire loops, which present the possibility of flow direction detection using this sensor. Aluminium wire sensors achieved an accuracy of 2.5%, in high flow regime, while platinum wire sensors had superior performance (0.06%) in low flows.

Numerous miniaturized flow sensors have been developed for monitoring biomedical signals, such as blood or intraocular pressure, intravascular blood flow, aspirated- and inspired-air flow, and breathing characteristics [52–55]. In this regard, an implantable catheter flow sensor established by Shikida et al., which was specified to sense breathing parameters of animal models after anchoring in the airway by means of legs [56]. The instrument was fabricated by insertion of patterned of an Au/Cr hot-film anemometer sensor into a heat shrinkable Teflon tube. It was evaluated inside the bronchus of a rabbit (Fig. 1.B).

Even with the substantial development of hot-film sensors, the devices still suffer from heat losses in the membrane on which the hot wire is deposited. Various materials have so far have been used to address this issue such as silicon nitride [57], or flexible polymers [58,59]. Nonetheless, these sensors are often used for flow separation detection and wall shear stress measurement as they are robust and easy to mount flush to a surface. More recently, De Luca et al. designed a CMOS thermoelectronic flow sensor based on five central hot-wire resistors made of tungsten inserted into a fully Si_3N_4- SiO_2 dielectric membrane to make a highly sensitive MEMS chip (Fig. 1.C) [60]. Hot-wire sensors are generally free from the substrate which enables an optimal heating uniformity and high sensitivity, but they are more fragile than hot-film sensors.

2.2. Calorimetric MEMS thermal flow sensors

Calorimetric flow sensors use two or more thermal sensors placed around a heater measure the temperature asymmetry caused by the passing fluid. Therefore, this method measure the velocity of fluid indirectly. Unlike hot-wire/hot-film sensors, calorimetric flow sensors show excellent performance in low flow rate measurement but they tend to saturate at higher flow rates, which limits their dynamic range. Depending on the material used to develop the sensing element, these sensors can be divided into two general categories of silicon and metallic forms (Table 2).

2.2.1. Silicon-based calorimetric MEMS thermal flow sensors

To protect fragile sensing elements, a silicon MEMS chip sensor was enclosed by Bruschi et al. in a PMMA cylinder composed of a specific configuration of channels. With this structure, the wind speed and direction be calculated via monitoring the distribution of airflow pressure by two distinct classical microcalorimeters [81]. Subsequently, this device was further miniaturized by integrating two thermal microstructures into a single chip using a commercial microelectronic process [82]. Furthermore, a more recent analytical study suggested two-dimensional directional anemometers based on fluidic structures capable of averaging the differential pressure developed by the wind across distinct diameters of the cylinder for flow direction detection [83]. In order to economically monitor nitrogen flow, Xu et al. reported a Temperature-compensated Thermoresistive Micro Calorimetric Flow (T2MCF) sensor, fabricated using a commercially available 0.35 μm 2P4M (two-poly layers, 4 metal layers) CMOS MEMS technology [84]. In this structure, the central polysilicon micro heater is constantly warmed, and modification of the fluid's thermal profile is monitored precisely by three pairs of thermoresistive sensors composed of polysilicon and aluminium layers.

2.2.2. Metallic-based calorimetric MEMS thermal flow sensors

One of the first studies in development of metallic-based calorimetric flow sensors was conducted by Ernst et al. who developed a high resolution Bio-MEMS device that was able to measure flow rates down to 100 nL/h, particularly for low thermal stable medical and biological liquids [85]. The sensor was made up of a 1.4 μm thick silicon nitride membrane on which all sensor structures were arranged and covered with a low temperature 700 nm plasma-enhanced chemical vapor deposition (PECVD) nitride layer. Later on, to achieve a wide range of detection, Sabaté et al. employed three pairs of sensing elements on a thin Si_3N_4 membrane [86].

Another study conducted by Dijkstra and colleagues developed a calorimetric miniaturized thermal flow sensor that was capable of detecting low liquid flow rates accurately [87]. The sensor consisted of a freestanding surface microchannel and a micro heater. The flow velocity was found by measuring the change in resistance between two upstream and downstream resistors due to the temperature disturbance. The sensor was tested for a range of DI water flow rates ranging from 0 $\mu L\,min^{-1}$ to 2 $\mu L\,min^{-1}$. The results demonstrated a linear response up to 300 $nL\,min^{-1}$ and a sensitivity of 218 $\mu V/(\mu L\,min^{-1})$.

In addition to mean flow measurements, shear-stress sensors can be used to measure the fluctuations of the wall shear stress on the surface [88]. This is particularly important when the flow state transitions from laminar to turbulent, or when the flow is fully turbulent. This is because the magnitude of wall shear stress in the turbulent boundary layer is larger than that in the laminar boundary layer [89]. However, these devices typically measure wall shear stress in order of Pascals, which is insufficient for most aerodynamic applications where the wall shear stress can be of the order of tens of Pascal or even much more when the flow speed is increased [88]. Generally, calorimetric flow sensors show excellent perfor-

Table 2
Calorimetric MEMS thermal sensors for detection of fluid flow rate and direction.

Sensing element material	Configuration	Fluid type	Detection range	Sensitivity	Ref
polysilicon heater n /p-polysilicon thermopiles	Calorimetric	Air	0.5–50 m/s	NA	[81]
P-polysilicon heater Al/p-polysilicon thermopile p-polysilicon/n-polysilicon thermopile	Calorimetric	Air	0.4–7.9 m/s	NA	[82]
P-doped polysilicon thermopile W/Ti heater	Calorimetric	Air	0–50 m/s	Silicon substrate: 3.04×10^{-2} V/(m/s) Soldered: 5.1×10^{-4} V/(m/s) Adhesive bonded: 2.01×10^{-2}V/(m/s)	[100]
Pt heater and detector	Calorimetric	Air	0–10 m/s	NA	[95]
Pt resistors	Calorimetric	Air	0–4×10^{-3} m/s	1.44×10^{-2} V/(m/s)	[87]
Ni resistors	Calorimetric	Air	0–1.4 m/s	NA	[93]
Si_3 N_4 membrane	Calorimetric	Air	NA	NA	[92]
Ge resistors Ti/Au/Ti heater	Calorimetric	Air	0.005–0.1 m/s	116.38 V/(m/s)W	[101]
Ti/Pt resistor	Calorimetric	Air	0–25 m/s	3.04×10^{-2} V(m/s)$^{-1/2}$	[98]
Ti/Pt resistor	Calorimetric	Air	0–30 m/s	0.164 K/(m/s)	[99]
Ni resistor	Calorimetric	Air	0–30 m/s	2.93×10^{-2} V/(m/s)	[94]
Pt resistor	Calorimetric	Air	5–25 m/s	50– 225 K/(m/s)	[88,102]
Cr/Pt resistive	Calorimetric	Air	0.016–0.167 m/s	9.4×10^{-3} V/(m/s)	[96]
Pt resistor	Calorimetric	Air	0–33 m/s	NA	[97]
Poly-Si micro heater Al/poly-Si thermocouple	Calorimetric	Gas, N2	0–11 m/s	230 V/(m/s)/W	[84]
Ti/Ni resistor	Calorimetric	Gas, N_2	3–237 m/s	1.35×10^{-3} V/(m/s)	[86]
SOI wafer CMOS wafer	Calorimetric Hot-wire/film	Gas, N2	0–73 m/s	NA	[71]
Pt thermistors	Calorimetric	Gas	0.5–1.5 m/s	NA	[103]
Pt thermistors	Anemometric Calorimetric	Gas	0.05–10 m/s	NA	[73]
Pt sensing element	Calorimetric	DI water	0–0.01 m/s	2.137 V/(m/s)	[76]
W/Ti/Pt sensing element	Calorimetric	DI water	1.33×10^{-2} m/s	2.14×10^{-6} V/(m/s)	[78]
Al/Si heater Polysilicon thermopiles	Calorimetric	Liquid	0–0.058 m/s	NA	[53]
Ge thermistors Cr heater	Calorimetric	Low thermal stable liquids	0–1.4 m/s	NA	[85]
Luminescent sensor layer	Calorimetric	Liquid	4.5×10^{-4}–0.457 m/s	216.5 K/(m/s)	[104]

Al, Aluminum; Au, Gold; B, Boron; Cr, Chromium; Cu, Copper; DI water, Deionized water; Ge, Germanium; GPM, Gallons per minute; NA, Not available data; Ni, Nickle;; Pt, Platinum; Re. No: Reynolds numbers Si, Silicon;; Si_3N_4, Silicon nitride; SOI, Silicon-on-insulator, Ti, Titanium; W, Tungsten.

mance with high sensitivity at low flow velocity measurements but tend to saturate at higher flow rates and thus suffer from limited dynamic range [90]. There have been several efforts reported in the past to improve the performance of flow sensors by combing two sensing principles such as calorimetric principle to hot-wire or hot-film to enable both increase of the sensitivity at low frequency and extension of measured flow range; thereby enabling higher signal to noise ratio over a wide dynamic range [90,91].

The MEMS thermal flow sensor was further developed by Hedrich et al. by producing a sensor that operated on a calorimetric principle that was suitable for sensing rapid flow velocity in spirometric applications with high accuracy, short response time and low power consumption at higher pressures [92]. They applied a venturi nozzle for measurement of turbulent breathing flow and formed a uniform flow over nozzle by the implementation of mesh screens at both sides of the sensing part. The sensor was composed of a thick low-pressure chemical vapour deposition (LPCVD) silicon nitride layer on a thin oxide as the membrane material, which was located on a silicon flow sensor chip. To prevent high-temperature disturbing effects, the sensor chip was enclosed in a metal head with a fluid channel used as a bypass. The metal head was designed to favour laminar flow and the silicon chip was located coplanar to the housing in order to avoid turbulence in the bypass channel. Fig. 1.D illustrates the schematic diagram of the sensor structure.

In another study, a microchannel integrated flow sensor was presented by Yu et al. to enhance flow measurement accuracy [93]. The flow sensor operated based on the calorimetric principle and consisted of a heater between two sensing elements on a diaphragm. Flow velocity was monitored by measuring the temperature difference between the two sensing elements. In this work, a microchannel was constructed under the diaphragm to allow air to flow on both sides of the diaphragm in order to generate forced convective thermal transfer between the diaphragm and the fluid. The flow sensor consisted of a Si_3N_4 and SiO_2 diaphragm, nickel resistors as heater and sensing elements, mounted on a silicon substrate base. Measurements showed a temperature difference between upstream and downstream sensing elements of 38.6 K for flow velocity of 3 m/s. In [94] an innovative strategy was used to improve the efficiency of thermal wind sensors. This was based on fabrication of trenches on a silicon substrate by deep reactive ion etching (DRIE) [94]. As a perspective view of the chip shows in Fig. 1.E, insulation spaces between a heater and eight thermistors minimized the lateral heat convection, and along with full-bridge measurement configuration, achieved higher performance.

There have been several attempts at developing thermal flow sensors to detect both flow velocity and direction. In the research conducted by Kim et al. [95], a circular thermal flow sensor was developed to measure both flow velocity and direction. This was implemented by fabrication of a silicon dioxide layer on the silicon diaphragm and forming a gap between heater and detectors. The flow velocity was measured from the power needed to overcome the temperature gradient of flow. The sensitivity of the sensor was determined to be 14 $\mu V/^{\circ}$. In addition, Li et al. developed a five-wire micro-fabricated anemometer with 3D directionality based on the calorimetric principle to detect low flow velocities and flow directionality [96]. They could achieve a velocity sensitivity of 9.4 mV/sm, with a relative direction sensitivity of 37.1 dB. Relative direction sensitivity is the minimum directional sensitiv-

ity of the sensor, which was calculated using the polar coordinate plot of relative sensitivity as a function of flow direction. In addition, Ye et al. show a significant improvement in the accuracy of their developed thermal flow sensor by increasing the number of heaters and thermistors in their device [97].

Zhu et al. fabricated a thermal wind sensor for low power application, capable of detecting wind direction with an accuracy of 6°, and whose total power consumption was only 24.5 mW (subsequently improved to 20 mW) [98]. The sensitivity of this system was further improved by decreasing the thickness of the glass substrate using wet etching process, the enhancement principally due to the lower conductive but higher convective heat transfer [99].

Moreover, in the literature there are a few studies intended to compare different thermal sensing strategies in micromachined devices. Meng et al. designed a parylene MEMS thermal sensor array that was able to detect small flow velocities by applying three popular flow sensing methods (hot film, calorimetric, and time-of-flight) [76,78]. The sensor consisted of seven platinum sensing elements arranged in a linear array, which were suspended in a Parylene C membrane on one side of a micromachined channel for measurements of hot-film mode. Fig. 1.F illustrates the schematic diagram of the parylene thermal flow sensor. The sensor utilized the heat transfer principle with three different modes of action. Through (i) constant temperature and (ii) constant current hot film methods, the convective heat loss from the heated resistive sensor was measured. While (iii) the calorimetric method utilized at least two sensing elements as upstream and downstream sensors and one heater to monitor the temperature profile displacement around a heating element in the presence of fluid flow. Fig. 1.F compares key parameters of the sensor for different modes of action, with calorimetric techniques showing the best resolution in low flow rates. Xu et al. have developed an advanced dual-mode micro thermal flow (DMTF) sensor that provides a great capability for wireless measurement of gas flow [71]. Through the combination of C-Type and H-Type modes, the DMTF system could support a flow range of 0–73 m/s of N2. Fig. 1.G shows the schematic view, photograph, and SEM image of a DMTF sensor using InvenSense 0.18 μm CMOS MEMS technology. This device opens up the possibility of using IoT (Internet of Things) techniques for energy monitoring of buildings.

Another interesting strategy to indirectly monitor the behavior of unsteady flows adjacent to a wall surface is focused on sensing of shear stress using the high-frequency response of thermal film sensors [59]. Several self-made MEMS thermal film sensors were applied to flexible skins, which provided a great ability for flow measurement, independent of any calibration processes and drift issues [63,64,105]. One of the interesting studies in this area has been done by Leu et al. who fabricated a miniaturized flexible vertical axis wind turbine (VAWT) to analyze types of unsteady flow in the boundary layer on pitching airfoils [58].

2.3. Challenges and perspectives on MEMS thermal flow sensors

In general, thermal flow sensors are considered as the most popular sensor type for monitoring velocity and direction, due to their low-cost, reliability, and higher accuracy. MEMS technology offers the ability to develop low-cost, scalable, and small device footprint thermal flow sensors with high sensitivity for both liquid and gas applications. These sensors, due to their high sensitivity, robustness, accuracy and fast response rate, have significant applications in area such as aviation, automation, oil and gas, which are challenging to measure with other technologies. MEMS-thermal flow sensors application is often limited to a non-corrosive environment to prevent them from degradation and avoid irreversible damage. There have been some efforts to develop thermal flow sensors for a harsh environment such as in gasoline and diesel by protecting the sensor using silicon carbide [106].

Another known issue with thermal flow sensor was the disability to accurately measure low flow velocities. Several platforms in design and fabrication of micro-electronic based devices have been suggested to overcome pivotal limitations of traditional thermal flow sensors, namely for monitoring gas flow in low velocities. Most thermal wind sensors rely on reducing the unwanted heat conduction in the chip in order to maximise the temperature difference produced by the airflow. These methods include etching the substrate to form an insulation trench [94], suspending the sensing element on membrane [101], and fabricating the device on a low thermal conductivity substrate [67]. Furthermore, the heat loss increases the power consumption and reduces the device sensitivity. To eliminate this issue, several improvements have been reported on MEMS- heat flow sensors on developing thermocouples and mesh-membrane structure [19,32,40,79].

Despite the impressive developments in fluid flow sensing using MEMS thermal sensors, there are still some concerns which limit their commercialization opportunities, including undesirable heat conduction, complex fabrication processes and poor sensitivity at low flow rates [107]. Several strategies have been employed to improve these factors which are mainly concentrated on the reduction of undesired thermal conductivity of the substrate by modification of the silicon layer or by using alternative materials with a lower thermal conductivity [51,75,94,98,101]. In practice, these improvements often resulted in fragile devices, which reduced the yield and compromised the potential for large scale production. To overcome this drawback, Shaun et al. reported a pillar-like microstructure on the silicon-based chip with low thermal conductance and great sensitivity [79]. Also, a recent Eight Trigram's inspired sensor shows high accuracy through an innovative design, as shown in Fig. 1.H [107]. More details on MEMS thermal flow sensors can be found in [106,108].

3. MEMS piezoresistive flow sensors

Piezoresistive materials are those that exhibit a change in resistivity when subjected to external stress or strain. The applied strain changes the internal atomic and lattice positions of material and hence, changes its resistivity. Piezoresistive materials have been widely used in the development of MEMS/NEMS flow sensors in literature [109,110]. The ability of piezoresistive materials to change resistance in response to applied stress makes them attractive to use for flow sensing. In a flow sensor configuration, the change in resistance can be converted to a voltage, which varies with the flow velocity. In the past, piezoresistive flow sensors were investigated for use in various applications including air fluid flow monitoring [8] and water flow monitoring [111–113]. Most of the reported piezoresistive sensors can be categorised into cantilever (Table 3) or diaphragm structure (Table 4), which are reviewed in this section.

3.1. Cantilever MEMS piezoresistive flow sensors

The first type of MEMS piezoresistive flow sensor developed was the cantilever-based structure, mainly made from silicon by means of microfabrication processes (Fig. 2.A). As pioneer studies, Svedin et al. presented a lift-force silicon-based flow sensor that was designed for acceleration insensitivity [114,115]. The sensor structure consisted of two airfoil plates connected to a rigid center beam through two flexible, stress-concentrating beams for each plate. As a result of airflow, both plates experienced small deflection, which was then detected by the polysilicon piezoresistors and converted to flow velocity. In 2002, Su et al. presented a highly sensitive ultra-thin micromachined silicon cantilever flow sensor [116]. The sensor consisted of a silicon cantilever beam with a strain gauge resistor integrated into each cantilever arm. The deflection

Table 3
Cantilever MEMS piezoresistive sensors for detection of fluid flow rate and direction.

Material	Configuration	Fluid type	Detection range	Sensitivity	Ref
Ti/Al resistor	Cantilever	Air	0.01–0.03 m/s	NA	[123]
Polysilicon strain gauges Al resistor	Cantilever	Air	0–6 m/s	7.4×10^{-6} l/(m/s)^2	[114]
Au/Cr cantilever beam	Cantilever	Air	NA	NA	[124]
Al resistor PZT film disk	Cantilever	Air	0.7–21 m/s	$0.65–4.49 \times 10^{-5}$ 1/(m/s)^2	[116]
Cr/Pt piezoresistive Cr/Au electrode	Cantilever	Air	5–45 m/s	0.0284 Ω/(m/s)	[117]
P type Si piezoresistor	Cantilever	Air	20–40 m/s	0.204×10^{-3} V/(m/s)	[120]
SOI sensing cantilever	Cantilever	Air	2–20 m/s	NA	[122]
Polysilicon strain gauges Al resistor	Cantilever	Gas	0–70 l/min	7.4×10^{-6} l/(m/s)^2	[24]
single crystalline Si piezoresistor	Cantilever	Water	0–0.23 m/s	150–350 Ω/(m/s)	[118]
Membrane cantilever beam array	Cantilever	Water	0.3–3.5 m/s	NA	[121]
SOI sensor chip Stainless steel cantilever	Cantilever	Water	0.07–0.35 m/s	NA	[8]

Al, Aluminium; Au, Gold; Cr, Chromium; pcb); NA, Not available data; PI, Polyimide; Pt, Platinum; PZT, Pb(Zr, Ti)O3; Si, Silicon; SOI, Silicon-On-Insulator; Sio2, Silicon dioxide.

Table 4
Diaphragm MEMS piezoresistive sensors for detection of fluid flow rate and direction.

Sensing element material	Configuration	Fluid type	Detection range	Sensitivity	Ref
Si sensing membrane Au strain gaugeHA-MA hydrogel cupula	Non-polymeric hair cell	Air	0.1–1 m/s	NA	[136]
CNT coated nanofiber Au/Pd electrodes Glass microcapillary	Non-polymeric hair cell	Air	0–10 m/s	NA	[125]
NiCr strain gauge Cr/Au electrode	Polymeric hair cell	Air	0–30 m/s	6×10^{-5} 1/(m/s)	[140]
LCP sensing membrane Au piezoresistors	Polymeric hair cell	Air	0.1–10 m/s	3.695×10^{-3} V/(m/s)	[146]
PEDOT:PSS micro hair Pd reference electrode Au working electrode	Polymeric hair cell	Air	0.66–0.97 m/s	NA	[126]
LCP piezoresistive film Cr/Au strain gauges	Polymeric hair cell	Air	8–160 l/min	0.004 V/(1/min)	[9]
Si piezoresistive strain gauge Ti/Au electrode	Non-polymeric hair cell	Air Water	0–20 m/s 0–0.4 m/s	NA 6.98 V/(m/s)	[134]
Si substrate PDMS lamellas	Non-polymeric hair cell	Air Water	0.12–2.5 l/min 0.1–1 ml/min	NA	[151]
LCP sensing membrane Au strain gauge HA- MA hydro gel cupula	Polymeric hair cell	Air Water	0–9 m/s 0–0.5 m/s	4.34×10^{-3} V/(m/s) 0.077 V/(m/s)	[112,145]
LCP sensing membrane Au strain gauge	Polymeric hair cell	Air Water	0–10 m/s 0–0.4 m/s	0.9×10^{-3} V/(m/s) 0.022 V/(m/s)	[149]
LCP sensing membrane Au piezoresistor	Polymeric hair cell	Air/Water	NA	NA	[111]
B-doped Si piezoresistive	Non-polymeric hair cell	Water	0–1 m/s	NA	[144]
Si cantilever PEG hydrogel cupula	Non-polymeric hair cell	Water	0.075×10^{-3}–0.1 m/s	1.6×10^{-3} V/(m/s)	[137]
Si sensing membrane	Non-polymeric hair cell	Water	0.5 and 0.75 m/s	NA	[152]
Si cantilever Doped Si strain gauge	Non-polymeric hair cell	Water	down to 10^{-4} m/s	NA	[131]
Si deformable membrane	Non-polymeric piezoresistive	Water	0.09–53.07 m/s	NA	[110]
Si cantilever PEG hydrogel cupula	Non-polymeric lateral-line	NA	NA	NA	[138]
LCP sensing membrane Cr/Au piezoresistors	Polymeric hair cell	Water	0–0.6 m/s	NA	[147]
Polyurethane resistor Au electrode	Polymeric hair cell	Water	NA	NA	[141,142]
B-doped SOI piezoresistive	Polymeric hair cell	Water	0.6×10^{-3}–0.08 m/s	NA	[143]
LCP sensing membrane Au strain gauge	Polymeric hair cell	Water	1.7×10^{-2}–0.14 m/s	NA	[16]
LCP sensing membrane Au gauge strain	Polymeric hair cell	Water	0.05, 0.1, 0.2 m/s	90.5×10^{-3} V/(m/s)	[148]
PDMS dome-shape sensing membrane Cu electrode	Polymeric peizoresistive	Water	0.1–0.4 m/s	NA	[153]
LCP3850 sensing membrane Cr/Au gauge line	polymeric hair cell	Liquid	100–500 mL/h	NA	[150]

Ag, Silver; Al, Aluminium; Au, Gold; B, Boron; CBPDMS, Carbon black-PDMS Composite; CNT, Carbon nanotube; HA, Hyaluronic Acid; HA-MA, Hyaluronic acid methacrylic anhydride; LCP, Liquid crystal polymer; LED, Light-emitting diode; PCB, Printed circuit board; Pd, Palladium; PDMS, Poly-dimethyl siloxane; PEDOT:PSS, Poly(3,4-ethylenedioxythiophene): Poly(styrenesulfonate); Si, Silicon Ti, Titanium.

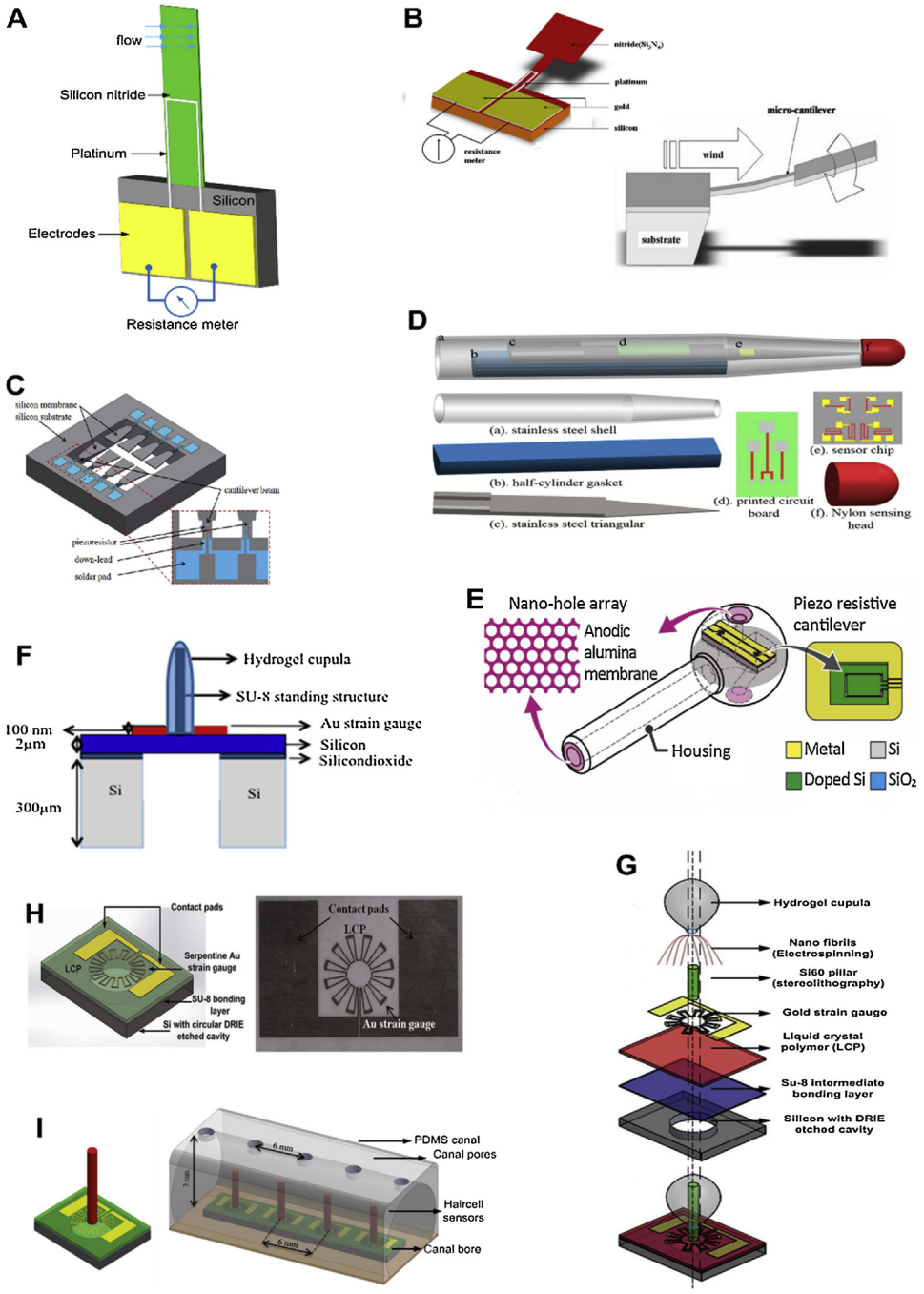

Fig. 2. MEMS piezoresistive flow sensors. (A) Basic structure of a MEMS flow sensor with a freestanding micro-cantilever structure. (B) Schematic illustration of a gas flow sensor (Upper figure) and its sensing operation diagram (Lower figure) [117]. (C) Schematic and detailed view of a cantilever water sensor formed by an array of inverted trapezoidal membranes [121]. (D) Schematic view of components of an SOI-based piezoresistive flow sensor [8]. (E) Schematic illustration of a waterproof airflow sensor designed to be used in to seabird bio-logging equipment [122]. (F) Schematic presentation of the general structure of a 3D polymer-based artificial neuromast sensor [136]. (G) Exploded drawing view of the main functional parts of the MEMS hair cell encapsulated in modified hyaluronic acid hydrogel cupula [112]. (H) Schematic presentation (not to scale) and top view photograph of individual micro-sensors be arranged in a lateral-line structure [148]. (I) Schematic drawing of a single hair cell structure (not to scale) and arrangement in a lateral line array [149].

and twist of the cantilever beam were measured by a piezoresistive strain gauge, and flow velocity determined from the strain gauge response. Furthermore, Wang et al. also developed a microcantilever flow sensor for air sensing [117]. The sensor consisted of a freestanding silicon microcantilever with a silicon nitride layer deposited on the silicon wafer and a platinum layer deposited on the silicon nitride to form a piezoresistive layer (Fig. 2.B). When the cantilever was subject to air flow past it, it was deflected downwards resulted in a change of resistance of the piezoresistive layer. The cantilever beams were produced in three different widths of 400 μm, 1200μm, and 2000μm for comparison. The cantilever beams with 2000 μm width demonstrated the highest sensitivity of 0.0284 Ω/m/s.

To measure a low flow rate with high sensitivity Zhang et al. fabricated a self-bent silicon microcantilever flow sensor [118]. This microcantilever sensor consisted of two silicon dioxide layers

constructed from silicon-on-insulator (SOI) wafers with a silicon piezoresistor sandwiched between the silicon dioxide layers. Water flow caused the microcantilever to bend due to drag and/or lift forces applied to the sensor, which leads to a change in resistance. Differential pressure sensors can detect flow rate based on the pressure difference between the upper and lower sides of cantilevers. Compared to traditional methods, applying piezoresistive component on cantilevers using micromachining techniques improved the sensitivity and resolution of detection, as reported by Takahashi et al. [119]. System simulation studies among various different shapes of paddles revealed the triangular forms had the highest sensitivity, due to the maximal stress generated [120]. However, Tian et al. reported the best numerical and modelling results for inverted trapezoidal membrane cantilever beam array (Fig. 2.C), in comparison to three common cantilever structure in MEMS flow sensors [121].

Given the importance of sensing ocean turbulence and monitoring water flow velocity, a Silicon on insulator (SOI)-based piezoresistive sensor has been constructed by Tian et al., which was composed of a nylon sensing head, stainless steel cantilever beam, SOI chip, printed circuit board, half-cylinder gasket, and stainless steel shell [8]. The simple schematic design of the main elements is presented in Fig. 2.D. Among different analysed structures, short triangular-long strip (STLS) cantilever and cylinder-ellipsoid (CYEL) nylon head produced the highest stress, so highest sensitivity in simulation tests. In general, the operation of the sensor was dependant on the deformation of the sensing head, which caused strain in the cantilever which was detected by four piezoresistive elements on SOI sensor chip.

A particular pitot tube-type sensor was fabricated by Takahashi et al. and was attached to a bio-logging system in order to monitor airflow velocity during seabird flight [122]. Apart from high sensitivity and low power consumption, the compact and waterproof construction of this sensor was promising for extensive use in studying seabird performance. As shown in Fig. 2.E, two SOI sensing cantilevers on a chip were combined to a nano-hole arrayed anodic alumina membrane in the tube inlets. Attachment of the membrane resulted in a reduction in sensitivity, but there was still sufficient remaining for the investigative purpose.

3.2. Diaphragm MEMS piezoresistive flow sensors

Scientists have long made considerable attempts to use nature as a model for innovation and problem-solving. In the last few years, more systematic studies are being conducted to understand various sensing mechanisms found in nature, for the purpose of introducing increasingly sophisticated capabilities to artificial sensor technology. Nature's materials and processes are often highly optimised. Each living creature is a laboratory that processes chemicals from the surroundings and produces multifunctional structures like bones, collagen, silk, leather, honey, wax, fur, etc. which are made through environmentally friendly processes with minimal waste, and result in strong, biodegradable and recyclable materials. [125]. The broad spectra of diaphragm-based piezoresistive sensors were invented through inspiration from biological flow sensors such as inner ear and outer ear hair cell and the lateral lines of blind cave fish, which greatly improved the performance of traditional flow sensors [126,127].

Given the interesting abilities of blind cavefish, a number of experiments have been conducted in the past to understand lateral line mediated behaviour of the species [38,128–130]. With awareness of surrounding flow velocities, pressure, and variations in each, the fish is able to perform rheotaxis, determine predator from prey, swim in schools, and navigate in the most energy efficient manner possible. Several biomimetic lateral-line structures have employed an array of artificial piezoresistive hair sensors mounted on a substrate to improve the efficiency of water flow measurement by detecting underwater pressure fluctuation [131].

In most bio-inspired sensors developed in the past, flow was measured by transferring the momentum induced on the hair cell by water flow, which caused deflection in the sensing membrane. The amount of deflection was usually measured by a strain gauge and converted to voltage output using a Wheatstone bridge circuit. Diaphragm-based piezoresistive flow sensors are generally characterized by the presence of a high aspect-ratio standing structure (perpendicular to the substrate plane). This configuration makes it possible to build a densely distributed array of flow sensors with minimal intrusion to the flow field, which distinguishes them from other non-biomimetic MEMS flow sensors. Various fabrication and assembly processes have been demonstrated for developing standing structures, which are generally composed of polymeric or non-polymeric sensing materials. They include wire bonding, plastic deformation magnetic assembly [124], 3D-printing [9], transfer moulding, and photolithographic patterning. The key point is that these structures should be robust to harsh underwater environment while being sensitive to the flow around it.

Various types of diaphragms for MEMS piezoresistive flow sensors have been developed for different application and sensing condition. Silicon-based membranes are sensitive and cost-effective materials with mature fabrication process, which are widely used in industrial and biomedical instruments [132]. On the other side, polymeric diaphragms are draw increasing attention according to their remarkable flexibility along with the notable biocompatibility, low-cost and different mechanical properties [133]. These types of piezoresistive MEMS flow sensors are reviewed in this section.

3.2.1. Non-polymeric diaphragm MEMS piezoresistive flow sensors

Silicon based piezoresistive flow sensors have been widely used due to their low-cost, and easy fabrication process. Such sensors often has a polymer component but the main diaphragm is made of silicone. For instance, Chen et al. used a high-aspect-ratio SU-8 epoxy cilium combined to a silicon strain gauge with a notable performance enhancement for using in biological applications [134]. However, the application of silicon-based sensors for some harsh submerged seawater conditions is limited, due to their fragile character. To address this problem, the sensor was casted into a polydimethylsiloxane (PDMS) polymer to form a robust tactile shear stress sensor [135]. Shear force caused the PDMS to bend and consequently bent the SU-8 hair cell enclosed in the PDMS, producing bending moment on the cantilever and change in the resistance of the piezoresistor. This robust sensor produced a linear response with sensitivity of 50 mV/KPa. They also fabricated a MEMS artificial neuromast hair cell sensor composed of three polymeric parts: (i) a sensing silicon membrane, (ii) SU-8 hair cell, and (iii) modified hyaluronic acid (HA) hydrogel cupula (Fig. 2.F) [136]. Compared to previously reported hair cells, this structure presented a higher sensitivity due to the full-bridge circuit on the membrane and the better mechanical and material properties of hyaluronic acid- methacrylic anhydride (HA-MA). The sensitivity of the hair cell flow sensors increases with the use of hydrogel cupula due to increase of the drag force and larger cross-sectional surface area exposed to flow in comparison to a naked hair cell, as well as the material properties of the hydrogel itself [137]. To develop a sensor more like an artificial cupula, Anderson et al. conducted a development of hydrogel cupula on the SU-8 hair cells in order to improve the sensitivity of patterned artificial hair cell sensors [138]. Poly-ethylene oxide acrylic macromonomer was used in the fabrication of hydrogel microstructures due to its ability to produce hydrogel of different shapes and sizes. Electrospun polycaprolactone microfibers were deposited onto the microfabricated hairs in

order to provide additional support for the hydrogel structures. The sensitivity of the hair sensor was predicted to increase by about twice that of the naked hair sensor.

3.2.2. Polymeric diaphragm MEMS piezoresistive flow sensors

It is shown that polymer based piezoresistive materials can have significant advantages in terms of gauge factor, sensitivity and durability as compare to silicon based sensors [139]. They also have lower moisture absorption rate, which makes polymer based flow sensors ideal for underwater sensing application. Such devices also offer interesting characteristics such wide range of elasticity and excellent chemical resistance. A primary artificial hair cell (AHC) airflow sensor was proceeded by Chen et al. on a substrate of polyimide film that protected a nichrome (NiCr) resistor and connected it to the cilium [140]. In 2006, Engel et al. reported an AHC device made entirely from polymers, mainly polyurethane [141,142]. This sensor was able to detect two-axis deflection of the vertical high aspect-ratio hair cell by utilizing four carbon-impregnated polyurethane force sensitive resistors (FSR), which were located on gold electrodes that measured the resistance.

Tucker et al. developed an artificial hair cell flow sensor consisting of a high aspect-ratio SU-8 cilium and a piezoresistive silicon cantilever [143]. This sensor operated by transferring the bending moment on the cilium to the cantilever, which produced strain at the base of the cantilever and caused change in resistance, similar to a previous work done by Fan et al. [144]. In 2016 the piezoresistive LCP flow sensor was further developed by Kottapalli et al. by introducing nanofibrils to bond the hydrogel cupula to the hair cells in order to enhance the sensitivity of flow sensing [112,145]. The exploded view of a hydrogel encapsulated hair cell sensor is presented in Fig. 2.G. The function of nanofibrils was to provide a good bonding between the cupula and the hair cell so that they were kept intact even for a high flow velocity beyond 1 ms^{-1}.

Kottapalli et al. [146–148] also developed a MEMS pressure sensor applied to flexible arrays used to measure flow for underwater surveillance. The individual sensor consisted of liquid crystal polymer (LCP) as the sensing membrane and a gold strain gauge, which are schematically shown in Fig. 2.H. Recently LCP has gained attention as an alternative to silicon for use as the sensing membrane, because of its better characteristics for underwater applications in terms of robustness, hermeticity, and fracture strength, as well as better sensitivity. The sensitivity measured was 90.5 mV/ms^{-1}, derived from water tunnel experiments.

Further improvement was made by introducing a hair cell on the sensor and an artificial canal neuromast [149] (Fig. 2.I). The hair cell made from Si60 formed by stereolithography was mounted on the LCP membrane at the centre of the gold strain gauge. The tall hair cell extended beyond the boundary layer generated by the flow, which enhanced the sensitivity of the sensor. The artificial canal neuromast developed in this work was fabricated from PDMS by the moulding process. The canal neuromast was a housing consisting of pores between the hair cells that were able to filter the steady-state flow. This significantly reduced the noise generated from the steady state and enhanced the detection of changes in the flows generated by moving underwater objects. The general sensing mechanism conducted by Kottapalli et al. [146] was also improved to measure the intravenous (IV) flow rate [150]. The gold nanolayer was patterned on top of the membrane to form a strain gauge and a hair cell was fixed in an IV tube by using a 3D printed fixture.

3.3. Challenges and perspective of MEMS piezoresistive flow sensors

MEMS piezoresistive flow sensors are becoming increasingly popular in chemical and biomedical applications due to their interesting characteristics such as biocompatibility, small size, low-power consumption and low-cost of fabrication [154]. Moreover, such sensors have shown excellent performance in low flow velocities monitoring [155]. Most reported piezoresistive sensors are inspired by the lateral line of blind cavefish [156,157] and are designed to offer similar characteristic as biological hair cells.

The performance of piezoresistive flow sensors can be influenced by temperature and humidity [158]. This problem became a critical challenge for using piezoresistive sensors in biomedical applications as their operational environment is predominantly vapour or liquid [151]. Particularly, in polymer piezoresistive sensors absorption of water moisture changes the mass of the sensing element matrix, which affects the mechanical stability, and accuracy of the sensor. In addition, MEMS piezoresistive flow sensors made with SU-8 resist components might be influenced by factors such as ageing of the SU-8 resist over time, which have adverse effects on both sensor performance, and durability of the sensors. There have been significant efforts reported in the literature to overcome these issues including by using solvent content [159] and optimising the fabrication process parameters [160].

4. MEMS piezoelectric flow sensor

Piezoelectricity is the property exhibited by some natural and synthetic dielectric materials, which develop surface distributions of electric charges when they are subjected to mechanical loads (direct piezoelectric effect) and, conversely, suffer geometric or dimensional changes when subjected to external electrical fields (converse piezoelectric effect) [161,162]. A significant piezoelectric effect can be observed in polycrystalline ferroelectric ceramics such as lead zirconate titanate (PZT) [161,162] or barium titanate (BaTiO3) [163] and polymers such as polyvinylidene fluoride (PVDF) [164,165], which are the most widely used in practical applications. Piezoelectric flow sensors are self-powered and hence, do not require a power supply to obtain the sensor output [166]. In the past, mainly two main materials were used in development of MEMS piezoelectric flow sensors which are lead zirconate titanate (PZT) and polyvinyledenedifluoride (PVDF). This section is dedicated to review these two types of MEMS flow sensors, which are summerized in Table 5.

4.1. PVDF-based MEMS piezoelectric flow sensors

PVDF exhibits impressive, mechanical and electrical characteristics such as piezoelectricity (highest amount the synthetic polymers), nonlinear optical properties and flexibility [167]. During the last decade, (PVDF) nanofiber has gained remarkable interest in many applications such as energy harvesting [168], tissue engineering [169] and sensors [170]. PVDF has coupled the piezoelectric characteristics of PVDF with the flexibility of the PDMS microfluidic channel presents a flexible gas flow sensing system with interesting potential for use in microfuel cells or biosensors [171]. Furthermore, PVDF show the capability to convert impulse pressure signals to electrical charges through the mechanical deformation of PVDF membrane. Another flexible flow sensor has been developed to monitor the blood flow rate of the portal vein during liver surgery [172]. It composed of a micro flow sensor fabricated on a spiral roll of polyvinyledenedifluoride–trifluoroethylene (PVDF-TrFE) piezoelectric copolymer. The thin PVDF-TrFE film also revealed a reliable response over a wide range of pressure and showed great potential for use in catheter devices for intravascular flow measurement [173].

To further improve the sensitivity of piezoelectric flow sensor, a sensor inspired by the mechanosensory ciliary bundles of fish has been developed by Asadnia et al. [174,175]. This artificial ciliary

Table 5
MEMS piezoelectric sensors for detection of fluid flow rate and direction.

Sensing element material	Configuration	Fluid type	Detection range	Sensitivity	Ref
Single PVDF sensing nanofiber Au electrode	Piezoelectric nanofiber	Air	NA	NA	[165]
PZT thin film	Piezoelectric pressure sensor	Air	NA	NA	[188]
Pyrex glass wafer Cr/Ti/Au electrode	Piezoelectric hair cell sensor	Air	0–8 m/s	NA	[193]
PZT sensing membrane Ti/Pt electrode	Piezoelectric hair cell sensor	Air Water	NA NA	0.82 V/(m/s) 0.22 V/(m/s)	[1]
PVDF piezoelectric PDMS channels	Piezoelectric pressure sensor	N2 gas	4.1×10^{-2}–2.87×10^{-4} m/s	NA	[171]
PVDF–TrFE piezoelectric film	Piezoelectric pressure sensor	water	14.86–42.46 m/s	4.8×10^{-5} V/(m/s)	[172]
PDMS micro-pillars PVDF nanofiber tip links HA-MA artificial cupula	Piezoelectric hair cell sensor	Water	10^{-6}m/s–8×10^{-2} m/s	0.3 V/(m/s)	[174,175]
PZT sensing membrane Ti/Pt electrode	Piezoelectric pressure sensor	Water	20–0.145 m/s	NA	[16]
Pb ($Zr_{0.52}Ti_{0.48}$)O3 piezoelectric thin film Gold electrode	Piezoelectric pressure sensor	Water	0.01–0.062 m/s	NA	[162] [161]
PZT sensing membrane Cr/Au electrode	Piezoelectric whisker sensor	Water	0–0.25 m/s	NA	[189]
PZT sensing membrane	Piezoelectric whisker sensor	Water	NA	NA	[30]
PDMS substrate PZT electrode	Piezoelectric lateral line sensor	Water	NA	NA	[111]
PZT sensing membrane HA-MA artificial cupula	Piezoelectric hair cell sensor	Water	NA	NA	[190]
ZnO transducers polyimide membrane	Piezoelectric pressure sensor	water	30–300 μl/h	2.08 (μL/h)/mV	[191]

ZnO, zinc oxide; PVDF, polyvinylidene fluoride; PDMS, polydimethylsiloxane; TrFE, Trifluoroethylene; PZT, Pb(Zr, Ti)O; HA-MA, hyaluronic acid-methacrylic anhydride hydrogel.

bundle was made up of 55 PDMS stereovilli arranged in 10 rows. The single tallest pillar known as kinocilium was located in the first row, followed by another 54 stereovilli arranged into 10 rows with decreasing height in which each stereovilli in the same row has the same height to each other (Fig. 3.B and 3.C). The tip links in the artificial stereovilli were formed by electrospinning piezoelectric polyvinylidene fluoride (PVDF) nanofibers. A hydrogel cupula was formed to cover the nanofibers in order to increase the sensitivity of the sensor as well as protecting the fragile nanofibers. The HA-MA hydrogel cupula increased the surface area and hence, increased the drag force. Furthermore, the increased height of the hair cells extended the structure beyond the boundary layer generated by the body in the flow, which consequently increase the sensitivity.

4.2. PZT-based MEMS piezoelectric flow sensors

Since the discovery of lead zirconate titanate (PZT) or [$Pb(Zr_{1-x},Ti_x)O_3$] and its subsequent extension into various compositions, there has been a continuous attention on using these composites in MEMS and micro-system technologies such as sensors and actuators. This is largely due to their intrinsic advantages such as strong piezoelectric effect, low power consumption, high-energy density, fast response, superior electrical properties and high Curie temperature [147,176–178]. Different methods have been invented for PZT ceramic and thin film fabrication such as sol-gel, mixing, grinding, calcination and forming method [179]. During the recent years, PZT have been fabricated as thick film [180–183] and thin film [184–187] in many MEMS devices. The best piezoelectric effect for PZT is reported around X = 0.52 also known as PZT(52/48), that is close to the morphotropic boundary. The airflow sensor designed by Tomimatsu et al. to manage wake-up signals in wireless sensor network (WSN) nodes applied a cantilever made up of a popular piezoelectric ceramic material, Pb(Zr, Ti)O3 (PZT) [188]. Any changes in airflow velocity around the sensor node caused vibration of the PZT, which in turn produced a voltage output and signaled the WSN to switch on. The schematic diagram of the flow sensor is presented in Fig. 3.D.

To improve situational awareness and obstacle avoidance, Asadnia et al. fabricated a PZT thin film piezoelectric pressure sensor array inspired by blind cavefish for underwater vehicles [161,162]. The sensor consisted of a PZT piezoelectric thin film with gold electrode sputtered on it, combined with a floating lower electrode for detection of very low frequency water disturbance. To form a flexible array of piezoelectric sensor, the sensors were packaged on a flexible LCP substrate with gold interconnects in an arrangement of 2 × 5 (Fig. 3.E).

Inspired by the blind cave fish, Asadnia et al. improved the previously developed piezoelectric pressure sensor by mounting a high aspect ratio artificial hair cell on the sensing membrane [1]. The sensor consisted of piezoelectric lead zirconate titanate (PZT) sensing membrane and flexible arrays of Si60 hair cells (Fig. 3. F). For flow measurement, disturbance of the water resulted in a pressure gradient across the hair cell, which consequently caused the bending of the hair cell. The bending moment was transferred to the piezoelectric membrane and generated an electric charge, producing a voltage output. Similar to the pressure sensor array, the artificial hair cell sensors were mounted on a LCP substrate to form a flexible array of sensors.

The piezoelectric flow sensor was further developed by introducing an artificial micro-whisker inspired by the whiskers on harbor seals. In the study conducted by Kottapalli et al. [30,189], the artificial piezoelectric seal whisker sensor consisted of the previously developed piezoelectric PZT sensing base and an artificial micro-whisker fabricated by stereolithography (Fig. 3.G). It was designed by having similar structure as the real seal whisker instead of a circular cylinder, with an elliptical cross-section and wave-like profiles on major and minor axes and variation of the offset angle along the length of the whisker. The unique geometry of the seal whisker was able to prevent the vortex-induced vibrations, which reduced noise in sensing low flow velocities.

A canal neuromast biomimetic piezoelectric MEMS flow sensor was fabricated by Bora et al., which revealed a good performance not only for oscillatory flow sensing but also in response to steady-state flows [190]. The rigid cylindrical Cu pillar was mounted on a PZT piezoelectric sensing membrane and fitted with a hydrogel

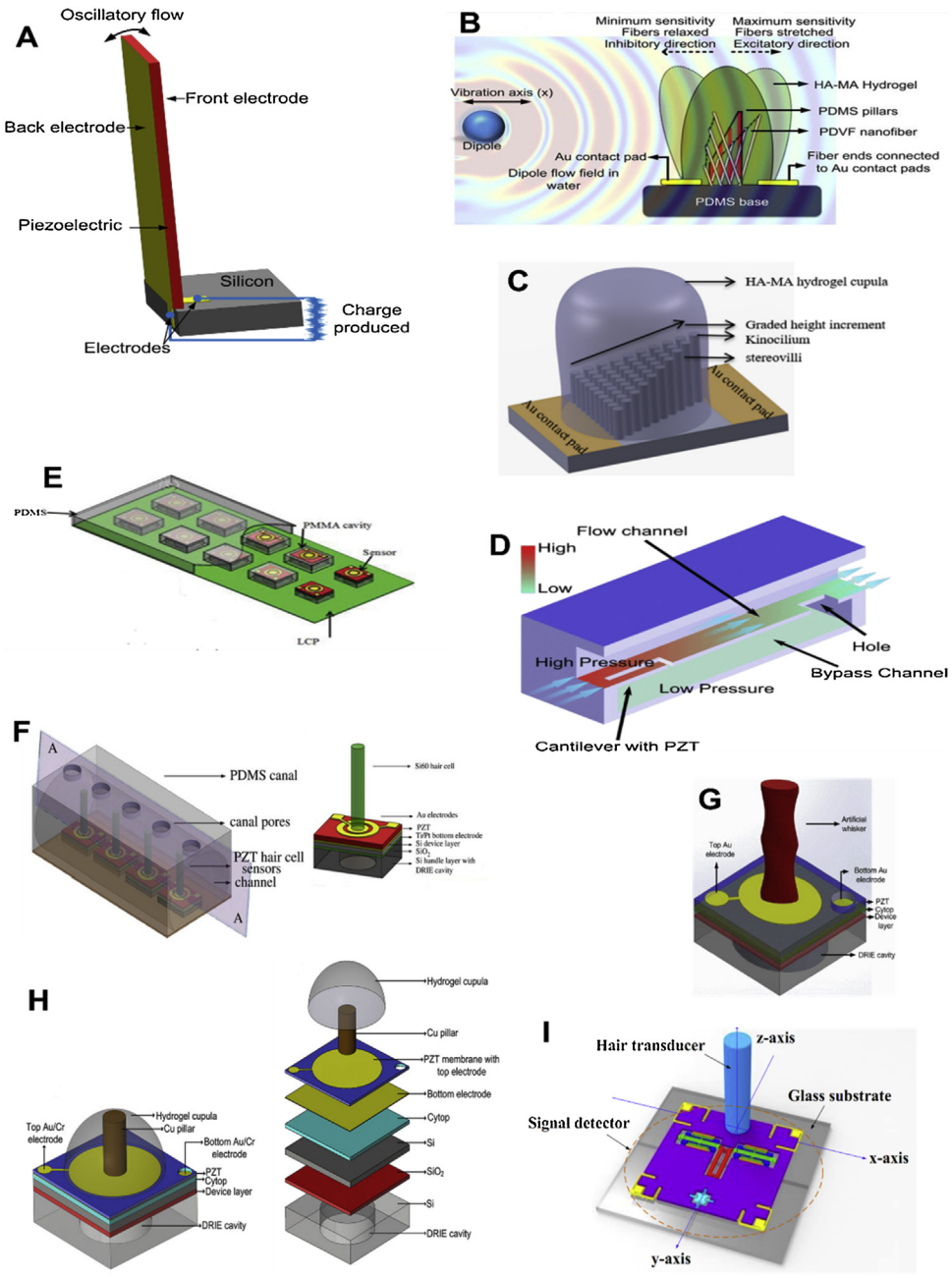

Fig. 3. MEMS piezoelectric flow sensors. (A) Basic structure of a MEMS micro cantilever piezoelectric flow sensor (B) Schematic presentation of the mechanism of flow sensing of bundle hair cell sensor [174] (C) And its design composed of different heights cilia connected to each other via PVDF nanofiber tip links and encapsulated by HA-MA hydrogel [175]. (D) Half-cut view of a piezoelectric flow sensor detecting air flow variation around wireless sensor nodes [188]. (E) Schematic drawing of flexible pattern of sensing elements on LCP membrane, which was waterproofed by a PDMS coating layer [162]. (F) Schematic array and detailed presentation of a single sensor structure of MEMS artificial fish skin [1]. (G) Schematic view of a piezoelectric hair cell sensor bioinspired from specific geometrical feature of harbor seal whiskers [189]. (H) Overall schematic figure and exploded drawing view of a MEMS-based flow sensor mimicked lateral line neuromasts of cavefish [190]. (I) Schematic structure of the particular asymmetric plan of a hair flow sensor works based on detecting resonant frequencies [193].

cupula (Fig. 3.H). The optimized HA-MA artificial cupula improved the mechanical properties of sensor that resulted in a higher sensitivity and robustness, in comparison to the bare structure. The nanofibers offer mechanical strength to the soft hydrogel cupula and enhance its endurance during underwater sensing applications. The artificial cupula sensors demonstrated a high increment in sensitivity of the sensor as compared to the naked hair cell sensors. Flow velocity and flow direction sensing in water is a more challenging task due to the requirement of waterproofing of the sensing elements and contacts of the sensor. The biomimetic approach together with the novel fabrication methods presented in this paper will form a guide to the development of nature-inspired micro- and nano- flow sensors in the future.

Apart from commonly use of PVDF and PZT in piezoelectric MEMS flow sensors, a differential pressure liquid flow sensor has been developed by Kuoni et al. [191]. This device is composed of a thin polyimide sheet thermally bonded to a silicon wafer as the sensor membrane and a ring shape zinc oxide (ZnO) piezoelectric

thin film as the sensing material. The flow sensing chip consisted of two pressure sensors with piezoelectric readout, which were connected to a hydraulic restriction. Flow was measured by detecting the pressure across the fluid, and applying conventional orifice plate meter flow meter calibration. Following the previous article by Tao et al. [192], a recent study has been focused on sensing airflow velocity by using a two-stage micro-leverage mechanism [193]. A single hair cell was asymmetrically bonded onto a pyrex glass wafer and the flow detected through measurement of frequency drifts of two symmetrically patterned resonators (Fig. 3.I). In comparison with alternatives, piezoelectric hair cell sensors offer a major advantage of being self-powered and hence of great benefit in space constrained UUV applications.

4.3. Challenges and perspective on MEMS piezoelectric flow sensors

Piezoelectric materials have been widely used in the development of sensors for sensing dynamic flow monitoring rather than static flow. Such sensors fail to detect static flow due to their large internal resistance which makes them unable to hold the sensor output [194], therefore they have often been used to measure oscillatory flows, detection of sound, generation of high voltages, electronic frequency generation and microbalances. Fig. 3.A illustrates the basic structure of a MEMS cantilever piezoelectric sensor. In this design, a piezoelectric material is sandwich between back and front electrodes enabling the sensor to receive the maximum amount of momentum and electric energy from the fluid or wind flow. These devices are typical Micromachines in the shape of a cantilever or thin microdiaphragm, which makes them fragile. There have been efforts to composite piezoelectric materials in polymer, which could render production of more robust piezoelectric flow sensors. On the other hand, piezoelectric devices are self-powered, which makes the experimental setup needless of using a power supply. This is due to the interesting behaviour of piezoelectric materials in response to a mechanical stress, which shifts the positive and negative charge centres in the material, which results in an external electric field. Although the piezoelectric coefficient PVDF is not as high as that of piezoelectric ceramics (such as PZT), PVDF is still one the interesting piezoelectric materials in MEMS/NEMS devices due to its high compliance, low thermal diffusivity and low permittivity [195].

5. Commercialisation avenues and challenges

MEMS flow sensors have a diverse range of applications ranging from industrial gas flow monitoring, environmental flow sensing, marine hydrodynamic sensing, and biomedical flow sensing applications. The small size, low-cost, high sensitivity, and batch fabrication compatibility of MEMS flow sensors make them very attractive for industrial and commercial applications. In addition, some of the soft polymer MEMS sensors reviewed in this manuscript are biocompatible, opening avenues for commercialization in biomedical and clinical applications.

There is a huge demand for MEMS flow sensors in clinical respiratory flow sensing applications such as sleep apnea diagnostic devices, ventilators, nebulizers, and oxygen supply systems. Wearable respiration monitors with embedded MEMS flow sensors capable of measuring flow velocities and flow rate are also in demand for athletic performance monitoring and rehabilitation monitoring. MEMS sensors would also play a quintessential role in flow velocity monitoring in intravenous infusions to allow accurate drug delivery in gravity based infusions and avoid accidental erroneous dosages which could be caused by infusion pump failures. Soft polymer and biocompatible MEMS flow sensors also pave the way for the development of implantable drug delivery systems. Conventionally, drug delivery is conducted through intravenous infusions, oral medication, pulmonary medication, or injections, all of which need regulated dosage as prescribed by the physician. The development of MEMS flow sensors, actuators, and micromachined micropumps and microvalves could lead to implantable drug delivery systems capable of accurately delivering drug dosages at desired time intervals. The major concern associated with commercialization of MEMS flow sensors within the biomedical domain is the use of soft polymer materials as sensing structures and sensing elements. While polymer MEMS has a high market demand in biomedical applications, owing to their biocompatibility not many polymer MEMS devices been commercialized as yet in comparison to silicon based devices. Repeatability, fast response, biocompatibility, wireless data acquisition, and high accuracy are current barriers to wide penetration of the polymer MEMS flow sensors in biomedical applications.

MEMS flow sensors are also in high demand for environmental wind flow velocity and flow direction monitoring for smart architecture and building design. Arrays of MEMS flow sensors embedded at various locations of a building provide constant monitoring of air circulation patterns within building complexes. Such information is useful to understand the heat distribution and thermal comfort for living in these dense housing complexes.

The past decade has seen a surge in the development of biomimetic MEMS flow sensors for hydrodynamic flow sensing. Inspired by the lateral-line sensors found in fishes, researchers have developed arrays of MEMS flow sensors which enable underwater vehicles to achieve artificial vision and energy-efficient manoeuvring. Such flow sensors are of great need in marine robotics and underwater/surface water vehicles where long term sensing with minimal human intervention is of interest. With the advent of biomimetic compact robots and swarm robots for surveillance in marine environment, there is an escalated demand for light-weight and flexible arrays of MEMS sensors for flow monitoring.

Flow sensors for pipeline leakage monitoring for both drinking water and oil bearing pipelines is another important application where the MEMS flow sensors reviewed in this work could have commercialization opportunities. Such pipelines can run for thousands of kilometers and need numerous flow meters at various points for reliable and efficient monitoring and detection of leakage locations, which can be very costly. Moreover, even if such large numbers of existing commercial flow meters are implemented, insertion flow meters available today interfere with the flow inside the pipe due to their large size. Despite the magnitude of the problem and the great need for flow sensors in pipelines, the commercialization of the MEMS flow sensors for this application has still been a challenge due to the stringent requirement for high robustness, remote sensing capability, and long term monitoring.

While a number of MEMS flow sensors are being developed through research activities, the sensing performance demanded by each application is unique, and depends on the environmental and flow parameters. Successful commercialization of the MEMS flow sensors reviewed in this manuscript requires significant developments in their capabilities of remote data acquisition, robustness and repeatability of sensing performance. Through this article, we only focused on three common types of MEMS flow sensors principles namely thermal, piezoeresistive and piezoelectric devices. There are however few reports on the other types of MEMS flow sensors such as capacitive [196–198], ultrasonic [199,200], coriolis flow meter [201–203], and turbine [23,204].

Fig. 4.A presents a distribution plot on the number of studies that have been performed on different types of MEMS flow sensors. Interestingly, just over a half (51.2%) of reports used the thermal sensing principle, with the calorimetric MEMS flow sensors slightly the most popular, but with similar numbers for thermal

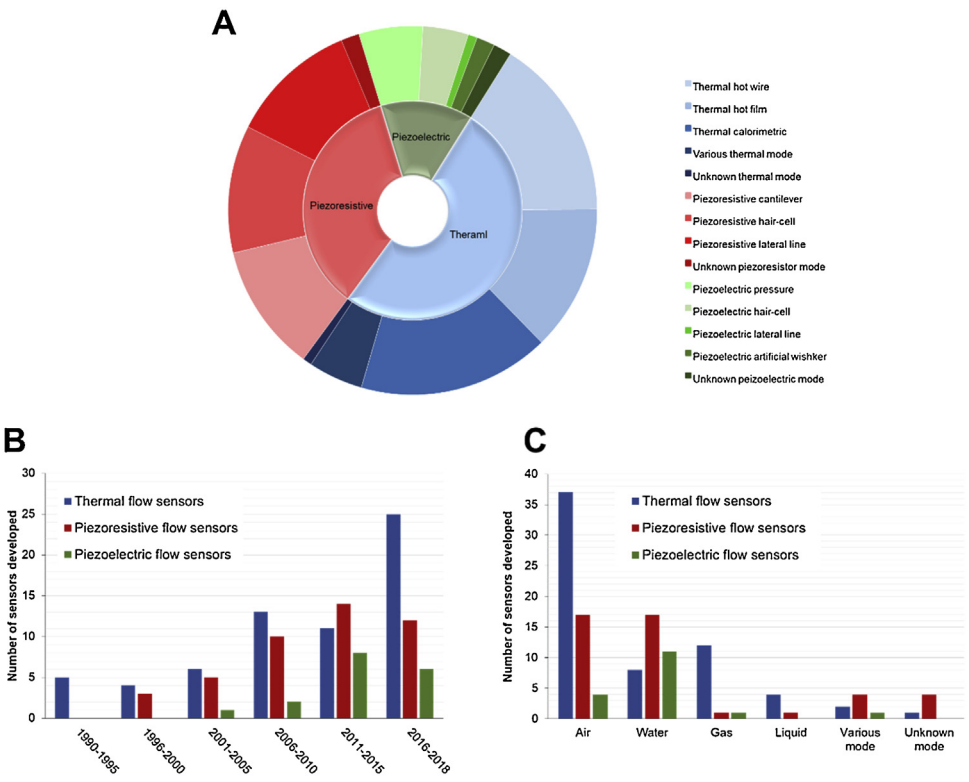

Fig. 4. The overall overview on research reports on MEMS flow sensors. (A) The pie chart of the proportion of various types of MEMS flow sensors with more details in second level. The categorization of MEMS flow sensors regarding (B) different time periods and (C) various fluid types.

hot-wire and hot-film systems. The second most common method, piezoresistive materials (35.2%), are interesting because of similar numbers for level for cantilever, hair cell, and lateral line MEMS flow sensors. Although the piezoelectric sensing mechanism has been used in the minority of studies (13.6%), it has attracted dramatic attention recently, as is seen in Fig. 4.B. However, it should be noted that the former studies in the field of MEMS flow sensors were mainly focused on thermal detection methods, which are still receiving attention currently. The piezoresistive flow sensors have been present since 1996, and were becoming the major strategy in this area during 2011-2015. We also found that thermal MEMS sensors were principally concentrated on airflow measurement, while piezoresistive systems were used for both air and water flow detection (Fig. 4.C). On the other hand, piezoelectric devices were applied to water flow sensing in the majority of studies.

Readout electronics associated with MEMS flow sensors could significantly affect the performance, sensitivity and cost of the sensory system. There have been several efforts of development of thermal flow meter with the read-out electronics integrated on the same chip [91,205] some of which have been commercialized [206]. These devices showed enhanced characteristics such as low response time and lower power consumption. Pitto et.al. developed a silicon chip including both the flow sensor and a configurable electronic interface to reduce the unavoidable offset of the sensing structures and the effect of pressure by means of the on-chip smart interface [206]. Recently, a readout integrated circuit (ROIC) was also reported to enable dual mode flow sensor on System on chips [207].

6. Concluding remarks

MEMS flow sensors offer numerous benefits compared to conventional flow sensors, including high spatial and temporal resolution, compact size, high sensitivity, and accuracy. With the aim of developing sensors with higher sensitivity, accuracy and threshold detection limit, researchers have investigated nature and developed biomimetic flow sensors. They learnt the sensing principles, morphological geometry, and design principles of the biological flow sensors in nature and applied them in developing artificial sensors using MEMS technologies. In this article, we have summarised the development of three main types of MEMS flow sensors including thermal, piezoresistive and piezoelectric devices and critically analysed their performance considering the material selection, sensitivity, application and design. A brief insight into various theories and working principles are detailed. The hot-wire/hot-film flow sensors exhibit good sensitivity over a large flow range but suffers from poor sensitivity at low flow rates. Piezoresistive flow sensors show excellent sensitivity at low flow velocity but they often require a power supply in order to bias the sensor in a wheatstone bridge configuration, allowing the voltage output generated due to the flow stimulus to be measured. The power supply presents difficulties for unmanned underwater robots (AUVs) and other underwater applications due to its size and weight. Therefore, a piezoelectric device for underwater flow sensing which provides a self-powered sensing ability is very attractive. In contrast, a hot-wire anemometer based design developed in the past performs flow sensing based on heat transfer and it will be challenging to use it for underwater sensing. Hair cells on torsional capacitive plates with thin gaps between moving plates are likely problematic for underwater applications, due to the complication of the narrow gap between the plates filling with water, and collapsing of the plates induced by capillary force. Finally, we cited existing challenges, outlooks and various applications of hot-wire, piezoresistive and piezoelectric MEMS flow sensors.

Acknowledgment

This work was supported By the Australian Research Council Centre Discovery Early Career Researcher Award (DECRA) DE180100688.

References

[1] M. Asadnia, A.G.P. Kottapalli, J. Miao, M.E. Warkiani, M.S. Triantafyllou, Artificial fish skin of self-powered micro-electromechanical systems hair cells for sensing hydrodynamic flow phenomena, J. R. Soc. Interface 12 (2015).

[2] C. Ghouila-Houri, Q. Gallas, E. Garnier, A. Merlen, R. Viard, A. Talbi, et al., High temperature gradient calorimetric wall shear stress micro-sensor for flow separation detection, Sens. Actuators A Phys. 266 (2017) 232–241.

[3] I. Etchart, H. Chen, P. Dryden, J. Jundt, C. Harrison, K. Hsu, et al., MEMS sensors for density-viscosity sensing in a low-flow microfluidic environment, Sens. Actuators A Phys. 141 (2008) 266–275.

[4] M. Gonzalez, H.R. Seren, G. Ham, E. Buzi, G. Bernero, M. Deffenbaugh, Viscosity and density measurements using mechanical oscillators in oil and gas applications, IEEE Trans. Instrum. Meas. 67 (2018) 804–810.

[5] H.M. Choi, B.R. Yoon, C.G. Kim, Y.M. Choi, Evaluation of flowmeters for heat metering, Flow Meas. Instrum. 22 (2011) 475–481.

[6] L. Lynnworth, Y. Liu, Ultrasonic flowmeters: half-century progress report, 1955–2005, Ultrasonics 44 (2006) e1371–e1378.

[7] G. de Graaf, A. Abarca, M. Ghaderi, R.F. Wolffenbuttel, A MEMS flow compensated thermal conductivity detector for gas sensing, in: G. Urban, J. Wollenstein, J. Kieninger (Eds.), Eurosensors 2015, 2015, pp. 1265–1268.

[8] B. Tian, H. Li, H. Yang, D. Song, X. Bai, Y. Zhao, A MEMS SOI-based piezoresistive fluid flow sensor, Rev. Sci. Instrum. 89 (2018), 025001.

[9] B. Abbasnejad, W. Thorby, A. Razmjou, D. Jin, M. Asadnia, M.E. Warkiani, MEMS piezoresistive flow sensors for sleep apnea therapy, Sens. Actuators A Phys. 279 (2018) 577–585.

[10] J. Bryzek, H. Abbott, A. Flannery, D. Cagle, J. Maitan, Control issues for MEMS, 42nd IEEE International Conference on Decision and Control, IEEE (2003) 3039–3047.

[11] C.-M. Ho, Y.-C. Tai, Micro-electro-mechanical-systems (MEMS) and fluid flows, Annu. Rev. Fluid Mech. 30 (1998) 579–612.

[12] G. Ciuti, L. Ricotti, A. Menciassi, P. Dario, MEMS sensor technologies for human centred applications in healthcare, physical activities, safety and environmental sensing: a review on research activities in Italy, Sensors 15 (2015) 6441–6468.

[13] R. Bogue, Recent developments in MEMS sensors: a review of applications, markets and technologies, Sens. Rev. 33 (2013) 300–304.

[14] S. Nihtianov, A. Luque, Smart Sensors and MEMS: Intelligent Devices and Microsystems for Industrial Applications, Woodhead Publishing, Amsterdam, The Netherlands, 2014.

[15] I.V. J. H. K, B.C. Claus, J.C. Kinsey, A navigation solution using a MEMS IMU, Model-Based Dead-Reckoning, and One-Way-Travel-Time acoustic range measurements for autonomous underwater vehicles, IEEE J. Ocean. Eng. (2018) 1–19.

[16] M. Asadnia, A.G.P. Kottapalli, R. Haghighi, A. Cloitre, P.V. y Alvarado, J. Miao, et al., MEMS sensors for assessing flow-related control of an underwater biomimetic robotic stingray, Bioinspir. Biomim. 10 (2015), 036008.

[17] S. Silvestri, E. Schena, Micromachined flow sensors in biomedical applications, Micromachines 3 (2012) 225–243.

[18] O. Sazhin, Liquid flow meter based on a thermal anemometer microsensor, J. Appl. Fluid Mech. 9 (2016) 1991–1996.

[19] V. Balakrishnan, T. Dinh, H.-P. Phan, D.V. Dao, N.-T. Nguyen, Highly sensitive 3C-SiC on glass based thermal flow sensor realized using MEMS technology, Sens. Actuators A Phys. 279 (2018) 293–305.

[20] A. Kottapalli, M. Asadnia, E. Kanhere, M. Triantafyllou, J. Miao, Smart skin of self-powered hair cell flow sensors for sensing hydrodynamic flow phenomena, Solid-State Sensors, Actuators and Microsystems (TRANSDUCERS), 2015 Transducers-2015 18th International Conference on (2015) 387–390.

[21] C. Liu, J.-B. Huang, Z.A. Zhu, F. Jiang, S. Tung, Y.-C. Tai, et al., A micromachined flow shear-stress sensor based on thermal transfer principles, J. Microelectromech. Syst. 8 (1999) 90–99.

[22] M. Sheplak, V. Chandrasekaran, A. Cain, Characterization of a silicon-micromachined thermal shear-stress sensor, AIAA J. 40 (2002) 1099–1104.

[23] N. Svedin, E. Stemme, G. Stemme, A static turbine flow meter with a micromachined silicon torque sensor, J. Microelectromech. Syst. 12 (2003) 937–946.

[24] N. Svedin, E. Kalvesten, E. Stemme, G. Stemme, A new silicon gas-flow sensor based on lift force, J. Microelectromech. Syst. 7 (1998) 303–308.

[25] E. Kälvesten, C. Vieider, L. Löfdahl, G. Stemme, An integrated pressure—flow sensor for correlation measurements in turbulent gas flows, Sens. Actuators A Phys. 52 (1996) 51–58.

[26] T. Ebefors, E. Kalvesten, G. Stemme, Three Dimensional Silicon Triple-hot-wire Anemometer Based on Polyimide Joints, Eleventh Annual International Workshop on Micro electro Mechanical Systems an Investigation of Micro structures, Sensors, Actuators, Machines and Systems, IEEE, Heidelberg, Germany, 1998, pp. 93–98.

[27] J. Van Baar, R.J. Wiegerink, T.S. Lammerink, G.J. Krijnen, M. Elwenspoek, Micromachined structures for thermal measurements of fluid and flow parameters, J. Micromech. Microeng. 11 (2001) 311.

[28] M.J. McHenry, S.M. van Netten, The flexural stiffness of superficial neuromasts in the zebrafish (Danio rerio) lateral line, J. Exp. Biol. 210 (2007) 4244–4253.

[29] W.Y. Wang, X.M. He, X.B. Wang, M.M. Wang, K. Xue, A bioinspired structure modification of piezoelectric wind energy harvester based on the prototype of leaf veins, Sens. Actuators A Phys. 279 (2018) 467–473.

[30] A.G.P. Kottapalli, M. Asadnia, J.M. Miao, M.S. Triantafyllou, Harbor seal whisker inspired flow sensors to reduce vortex-induced vibrations, in: 2015 28th IEEE International Conference on Micro Electro Mechanical Systems (MEMS), February Ed., Estoril, Portugal, 2015, pp. 889–892.

[31] J. Zhang, L.F. Hao, F. Yang, W.C. Jiao, W.B. Liu, Y.B. Li, et al., Biomimic hairy skin tactile sensor based on ferromagnetic microwires, ACS Appl. Mater. Interfaces 8 (2016) 33848–33855.

[32] C.-H. Wu, D. Kang, P.-H. Chen, Y.-C. Tai, MEMS thermal flow sensors, Sens. Actuators A Phys. 241 (2016) 135–144.

[33] A. Cabrita, R. Mendes, D.A. Quintela, Thermistor based, low velocity isothermal, air flow sensor, Meas. Sci. Technol. 27 (2016).

[34] J.T. Kuo, L. Yu, E. Meng, Micromachined thermal flow sensors—a review, Micromachines 3 (2012) 550–573.

[35] B.W. van Oudheusden, Silicon thermal flow sensors, Sens. Actuators A Phys. 30 (1992) 5–26.

[36] C. Hung-Ming, T. Kong-Beng, T. Sheng-Fu, L. Wen-Chau, Temperature-dependent characteristics of polysilicon and diffused resistors, IEEE Trans. Electron Devices 50 (2003) 1413–1415.

[37] B.W. van Oudheusden, A.W. van Herwaarden, High-sensivity 2-D flow sensor with an etched thermal isolation structure, Sens. Actuators A Phys. 22 (1989) 425–430.

[38] D. Moser, R. Lenggenhager, H. Baltes, Silicon gas flow sensors using industrial CMOS and bipolar IC technology, Sens. Actuators A: Phys. 27 (1991) 577–581.

[39] E. Yoon, An integrated mass flow sensor with on-chip CMOS interface circuitry, IEEE Trans. Electron Devices 39 (1992) 1376–1386.

[40] G. Kaltsas, A.G. Nassiopoulou, Novel C-MOS compatible monolithic silicon gas flow sensor with porous silicon thermal isolation, Sens. Actuators A: Phys. 76 (1999) 133–138.

[41] B. Idjeri, M. Laghrouche, J. Boussey, Wind measurement based on MEMS micro-anemometer with high accuracy using ANN technique, IEEE Sens. J. 17 (2017) 4181–4188.

[42] S. Wu, Q. Lin, Y. Yuen, Y.C. Tai, MEMS flow sensors for nano-fluidic applications, Sens. Actuators A: Phys. 89 (2001) 152–158.

[43] R. Kersjes, W. Mokwa, G. Zimmer, H. Vogt, Flow Sensor Component, Fraunhofer Gesellschaft Zur Forderung Der Angewandten Forschung, 2002.

[44] A. Van der Wiel, C. Linder, N. De Rooij, A. Bezinge, A liquid velocity sensor based on the hot-wire principle, Sens. Actuators A Phys. 37 (1993) 693–697.

[45] R. Kersjes, J. Eichholz, A. Langerbein, Y. Manoli, W. Mokwa, An integrated sensor for invasive blood-velocity measurement, Sens. Actuators A Phys. 37 (1993) 674–678.

[46] T. Dinh, H. Phan, A. Qamar, P. Woodfield, N. Nguyen, D.V. Dao, Thermoresistive effect for advanced thermal sensors: fundamentals, design considerations, and applications, J. Microelectromech. Syst. 26 (2017) 966–986.

[47] L. Qiu, S. Hein, E. Obermeier, A. Schubert, Micro gas-flow sensor with integrated heat sink and flow guide, Sens. Actuators A: Phys. 54 (1996) 547–551.

[48] S. Pandya, Y. Yang, D.L. Jones, J. Engel, C. Liu, Multisensor processing algorithms for underwater dipole localization and tracking using MEMS artificial lateral-line sensors, EURASIP J. Appl. Signal Processing 2006 (2006) 1–8.

[49] J. Chen, Z. Jun, L. Chang, A surface micromachined, out-of-plane anemometer, in: Technical Digest MEMS 2002 IEEE International Conference Fifteenth IEEE International Conference on Micro Electro Mechanical Systems (Cat No02CH37266), 2002, pp. 332–335.

[50] S.C.C. Bailey, G.J. Kunkel, M. Hultmark, M. Vallikivi, J.P. Hill, K.A. Meyer, et al., Turbulence measurements using a nanoscale thermal anemometry probe, J. Fluid Mech. 663 (2010) 160–179.

[51] M. Sadeghi, R. Peterson, K. Najafi, Air flow sensing using micro-wire-bonded hair-like hot-wire anemometry, J. Micromech. Microeng. 23 (2013), 085017.

[52] M. Leonardi, P. Leuenberger, D. Bertrand, A. Bertsch, P. Renaud, A soft contact lens with a MEMS strain gage embedded for intraocular pressure monitoring, 12th International Conference on Solid-State Sensors, Actuators and Microsystems Digest of Technical Papers IEEE (2003) 1043–1046.

[53] B. Mimoun, A. Van Der Horst, R. Dekker, D. Van Der Voort, M. Rutten, F. van de Vosse, Thermal Flow Sensors on Flexible Substrates for Minimally Invasive Medical Instruments, Sensors, 2012 IEEE, IEEE, Taipei, Taiwan, 2012, pp. 1–4.

[54] M. Shikida, T. Shikano, T. Matsuyama, Y. Yamazaki, M. Matsushima, T. Kawabe, Micromachined catheter flow sensor and its applications in breathing measurements in animal experiments, Microsyst. Technol. 20 (2014) 505–513.

[55] M. Shikida, T. Yokota, T. Kawabe, T. Funaki, M. Matsushima, S. Iwai, et al., Characteristics of an optimized catheter-type thermal flow sensor for measuring reciprocating airflows in bronchial pathways, J. Micromech. Microeng. 20 (2010), 125030.

[56] M. Shikida, T. Matsuyama, T. Yamada, M. Matsushima, T. Kawabe, Development of implantable catheter flow sensor into inside of bronchi for laboratory animal, Microsyst. Technol. 23 (2017) 175–185.

[57] Y. Ou, F.R. Qu, G.Y. Wang, M.Y. Nie, Z.G. Li, W. Ou, et al., A MEMS thermal shear stress sensor produced by a combination of substrate-free structures with anodic bonding technology, Appl. Phys. Lett. 109 (2016).
[58] T. Leu, J. Yu, J. Miau, S. Chen, MEMS flexible thermal flow sensors for measurement of unsteady flow above a pitching wind turbine blade, Exp. Therm. Fluid Sci. 77 (2016) 167–178.
[59] J. Miau, T. Leu, J. Yu, J. Tu, C. Wang, V. Lebiga, et al., Mems thermal film sensors for unsteady flow measurement, Sens. Actuators A Phys. 235 (2015) 1–13.
[60] A. De Luca, C. Falco, E.L. Gardner, J.D. Coull, F. Udrea, Diode-based CMOS MEMS thermal flow sensors, 19th International Conference on Solid-State Sensors, Actuators and Microsystems (TRANSDUCERS) (2017) 2211–2214.
[61] S.-T. Hung, S.-C. Wong, W. Fang, The development and application of microthermal sensors with a mesh-membrane supporting structure, Sens. Actuators A Phys. 84 (2000) 70–75.
[62] J. Chen, C. Liu, Development and characterization of surface micromachined, out-of-plane hot-wire anemometer, J. Microelectromech.Syst. 12 (2003) 979–988.
[63] J.-J. Miau, J. Tu, J. Chou, G. Lee, Sensing flow separation on a circular cylinder by micro-electrical-mechanical-system thermal-film sensors, AIAA J. 44 (2006) 2224–2230.
[64] J.-J. Miau, J. Tu, T. Liao, Insights into vortex shedding with data analysis, J. Fluid Sci. Technol. 4 (2009) 415–429.
[65] Y. Hasegawa, H. Kawaoka, T. Yamada, M. Matsushima, T. Kawabe, M. Shikida, Respiration and heartbeat signal detection from airflow at airway in rat by catheter flow sensor with temperature compensation function, J. Micromech. Microeng. 27 (2017), 125016.
[66] H. Liu, N. Lin, S. Pan, J. Miao, L.K. Norford, High sensitivity, miniature, full 2-D anemometer based on MEMS hot-film sensors, IEEE Sens. J. 13 (2013) 1914–1920.
[67] S.W. Liu, S.S. Pan, F. Xue, L. Nay, J.M. Miao, L.K. Norford, Optimization of hot-wire airflow sensors on an out-of-Plane glass bubble for 2-D detection, J. Microelectromech. Syst. 24 (2015) 940–948.
[68] C. Ghouila-Houri, J. Claudel, J.C. Gerbedoen, Q. Gallas, E. Garnier, A. Merlen, et al., High temperature gradient micro-sensor for wall shear stress and flow direction measurements, Appl. Phys. Lett. 109 (2016).
[69] Y. Hasegawa, H. Kawaoka, Y. Mitsunari, M. Matsushima, T. Kawabe, M. Shikida, Catheter type thermal flow sensor with small footprint for measuring breathing function, Microsyst. Technol. 24 (2018) 1–11.
[70] H. Kawaoka, T. Yamada, M. Matsushima, T. Kawabe, Y. Hasegawa, M. Shikida, Detection of kinetic heartbeat signals from airflow at mouth by catheter flow sensor with temperature compensation, 2016 IEEE 29th International Conference on Micro Electro Mechanical Systems (MEMS) (2016) 359–362.
[71] W. Xu, B. Lijin, M. Duan, X. Wang, J. Wicaksana, A. Min, et al., A Wireless Dual-mode Micro Thermal Flow Sensor System With Extended Flow Range by Using CMOS-MEMS Process, IEEE Micro electro mechanical systems (MEMS), IEEE, Belfast, UK, 2018, pp. 824–827.
[72] S. Dong, S. Duan, Q. Yang, J. Zhang, G. Li, R. Tao, MEMS-based smart gas metering for internet of things, IEEE Internet Things J. 4 (2017) 1296–1303.
[73] N. Djuzhev, D. Novikov, G. Demin, A. Ovodov, V. Ryabov, An experimental study on MEMS-based gas flow sensor for wide range flow measurements, Sensors Applications Symposium (SAS), 2018 IEEE (2018) 1–4.
[74] H.H. Liao, A carrier gas flow velocity and flow direction sensor and its interface circuit, Appl. Mech. Mater. (2014) 542–549, Trans Tech Publ.
[75] R. Ahrens, K. Schlote-Holubek, A micro flow sensor from a polymer for gases and liquids, J. Micromech. Microeng. 19 (2009), 074006.
[76] E. Meng, Y.C. Tai, A parylene MEMS flow sensing array, TRANSDUCERS' 03 12th International Conference on Solid-State Sensors, Actuators and Microsystems Digest of Technical Papers Boston (2003) 686–689.
[77] Y. Yang, J. Chen, J. Engel, S. Pandya, N. Chen, C. Tucker, et al., Distant touch hydrodynamic imaging with an artificial lateral line, Proc. Natl. Acad. Sci. 103 (2006) 18891.
[78] E. Meng, P.Y. Li, Y.C. Tai, A biocompatible Parylene thermal flow sensing array, Sens. Actuators A: Phys. 144 (2008) 18–28.
[79] F. Shaun, S. Sarkar, F. Marty, P. Poulichet, W. César, E. Nefzaoui, et al., Sensitivity optimization of micro-machined thermo-resistive flow-rate sensors on silicon substrates, J. Micromech. Microeng. 28 (2018), 074002.
[80] K.K. Mistry, A. Mahapatra, Design and simulation of a thermo transfer type MEMS based micro flow sensor for arterial blood flow measurement, Microsyst. Technol. 18 (2012) 683–692.
[81] P. Bruschi, M. Dei, M. Piotto, A low-power 2-D wind sensor based on integrated flow meters, IEEE Sens. J. 9 (2009) 1688–1696.
[82] M. Piotto, G. Pennelli, P. Bruschi, Fabrication and characterization of a directional anemometer based on a single chip MEMS flow sensor, Microelectron. Eng. 88 (2011) 2214–2217.
[83] P. Bruschi, M. Piotto, Determination of the wind speed and direction by means of fluidic-domain signal processing, IEEE Sens. J. 18 (2018) 985–994.
[84] W. Xu, B. Gao, S. Ma, A. Zhang, Y. Chiu, Y.-K. Lee, Low-cost temperature-compensated thermoresistive micro calorimetric flow sensor by using 0.35 μm CMOS MEMS technology, IEEE 29th International Conference on Micro Electro Mechanical Systems (MEMS) (2016) 189–192.
[85] H. Ernst, A. Jachimowicz, G.A. Urban, High resolution flow characterization in Bio-MEMS, Sens. Actuators A: Phys. 100 (2002) 54–62.
[86] N. Sabaté, J. Santander, L. Fonseca, I. Gràcia, C. Cané, Multi-range silicon micromachined flow sensor, Sens. Actuators A Phys. 110 (2004) 282–288.
[87] M. Dijkstra, M.J. de Boer, J.W. Berenschot, T.S.J. Lammerink, R.J. Wiegerink, M. Elwenspoek, Miniaturized thermal flow sensor with planar-integrated sensor structures on semicircular surface channels, Sens. Actuators A Phys. 143 (2008) 1–6.
[88] J. Weiss, E. Jondeau, A. Giani, B. Charlot, P. Combette, Static and dynamic calibration of a MEMS calorimetric shear-stress sensor, Sens. Actuators A Phys. 265 (2017) 211–216.
[89] G.H. Ding, B.H. Ma, J.J. Deng, W.Z. Yuan, K. Liu, Accurate measurements of wall shear stress on a plate with elliptic leading edge, Sensors 18 (2018).
[90] J.T.W. Kuo, L. Yu, E. Meng, Micromachined thermal flow Sensors-A review, Micromachines 3 (2012) 550–573.
[91] M. Ahmed, W. Xu, S. Mohamad, F. Boussaid, Y.K. Lee, A. Bermak, Fully integrated bidirectional CMOS-MEMS flow sensor with low power pulse operation, IEEE Sens. J. 19 (2019) 3415–3424.
[92] F. Hedrich, K. Kliche, M. Storz, S. Billat, M. Ashauer, R. Zengerle, Thermal flow sensors for MEMS spirometric devices, Sens. Actuators A Phys. 162 (2010) 373–378.
[93] B. Yu, Z. Gan, S. Cao, J. Xu, S. Liu, A micro channel integrated gas flow sensor for high sensitivity, in: 2008 11th IEEE Intersociety Conference on Thermal and Thermomechanical Phenomena in Electronic Systems, I-THERM, 2008, pp. 215–220.
[94] Y. Ye, Z. Yi, S. Gao, M. Qin, Q.-A. Huang, DRIE trenches and full-bridges for improving sensitivity of 2-D micromachined silicon thermal wind sensor, J. Microelectromech. Syst. 26 (2017) 1073–1081.
[95] S. Kim, T. Nam, S. Park, Measurement of flow direction and velocity using a micromachined flow sensor, Sens. Actuators A Phys. 114 (2004) 312–318.
[96] Z. Li, W.H. Chang, C.C. Gao, Y.L. Hao, A novel five-wire micro anemometer with 3D directionality for low speed air flow detection and acoustic particle velocity detecting capability, J. Micromech. Microeng. 28 (2018).
[97] Y.Z. Ye, Z.X. Yi, S.X. Gao, M. Qin, Q.A. Huang, Octagon-shaped 2-D micromachined thermal wind sensor for high-accurate applications, J. Microelectromech. Syst. 27 (2018) 739–747.
[98] Y.-q. Zhu, B. Chen, M. Qin, J.-q. Huang, Q.-a. Huang, Development of a self-packaged 2D MEMS thermal wind sensor for low power applications, J. Micromech. Microeng. 25 (2015), 085011.
[99] Y.Q. Zhu, M. Qin, J.Q. Huang, Z.X. Yi, Q.A. Huang, Sensitivity improvement of a 2D MEMS thermal wind sensor for low-power applications, IEEE Sens. J. 16 (2016) 4300–4308.
[100] H. Sturm, W. Lang, Membrane-based thermal flow sensors on flexible substrates, Sens. Actuators A Phys. 195 (2013) 113–122.
[101] A.S. Cubukcu, E. Zernickel, U. Buerklin, G.A. Urban, A 2D thermal flow sensor with sub-mW power consumption, Sens. Actuators A Phys. 163 (2010) 449–456.
[102] J. Weiss, Q. Schwaab, Y. Boucetta, A. Giani, C. Guigue, P. Combette, et al., Simulation and testing of a MEMS calorimetric shear-stress sensor, Sens. Actuators A Phys. 253 (2017) 210–217.
[103] N.A. Djuzhev, D. Novikov, V. Ryabov, Application of the Streamlined Body for Properties Amplification of Thermoresistive MEMS Gas Flow Sensor, Solid State Phenomena, Trans Tech Publ, 2016, pp. 247–252.
[104] C. Hoera, M.M. Skadell, S.A. Pfeiffer, M. Pahl, Z. Shu, E. Beckert, et al., A chip-integrated highly variable thermal flow rate sensor, Sens. Actuators B Chem. 225 (2016) 42–49.
[105] D. Mironov, Investigation of Flow Over Shallow Cavity Using Wavelet and Hilbert-huang Yransform, National cheng kung university, Tainan, Taiwan, 2008.
[106] V. Balakrishnan, H.P. Phan, T. Dinh, D.V. Dao, N.T. Nguyen, Thermal flow sensors for harsh environments, Sensors 17 (2017).
[107] Y. Ye, Z. Yi, M. Qin, Q.-A. Huang, Eight-trigram-inspired MEMS Thermal Wind Sensor With Improved Accuracy, IEEE Micro electro mechanical systems (MEMS), IEEE, Belfast, UK, 2018, pp. 836–839.
[108] V. Balakrishnan, T. Dinh, T. Nguyen, H.P. Phan, T.K. Nguyen, D.V. Dao, et al., A Hot-film Air Flow Sensor for Elevated Temperatures, Review of Scientific Instruments, 2019, pp. 90.
[109] A.A. Barlian, W.-T. Park, J.R. Mallon, A.J. Rastegar, B.L. Pruitt, Semiconductor piezoresistance for microsystems, Proceedings of the IEEE 97 (2009) 513–552.
[110] P. Sharma, J.F. Motte, F. Fournel, B. Cross, E. Charlaix, C. Picard, A Direct sensor to measure minute liquid flow rates, Nano Lett. 18 (2018) 5726–5730.
[111] E. Kanhere, N. Wang, A.G.P. Kottapalli, M. Asadnia, V. Subramaniam, J.M. Miao, et al., Crocodile-inspired dome-shaped pressure receptors for passive hydrodynamic sensing, Bioinspir. Biomim. 11 (2016).
[112] A.G.P. Kottapalli, M. Bora, M. Asadnia, J. Miao, S.S. Venkatraman, M. Triantafyllou, Nanofibril scaffold assisted MEMS artificial hydrogel neuromasts for enhanced sensitivity flow sensing, Sci. Rep. 6 (2016).
[113] J.E. Dusek, M.S. Triantafyllou, J.H. Lang, Piezoresistive foam sensor arrays for marine applications, Sens. Actuators A Phys. 248 (2016) 173–183.
[114] N. Svedin, E. Stemme, G. Stemme, New bi-directional gas-flow sensor based on lift force, in: International Conference on Solid-State Sensors and Actuators, Proceedings, 1997, pp. 145–148.
[115] N. Svedin, E. Kälvesten, E. Stemme, G. Stemme, A lift-force flow sensor designed for acceleration insensitivity, Sens. Actuators A Phys. 68 (1998) 263–268.

[116] Y. Su, A.G.R. Evans, A. Brunnschweiler, G. Ensell, Characterization of a highly sensitive ultra-thin piezoresistive silicon cantilever probe and its application in gas flow velocity sensing, J. Micromech. Microeng. 12 (2002) 780–785.
[117] Y.H. Wang, C.Y. Lee, C.M. Chiang, A MEMS-based air flow sensor with a free-standing microcantilever structure, Sensors 7 (2007) 2389–2401.
[118] Q. Zhang, W. Ruan, H. Wang, Y. Zhou, Z. Wang, L. Liu, A self-bended piezoresistive microcantilever flow sensor for low flow rate measurement, Sens. Actuators A Phys. 158 (2010) 273–279.
[119] H. Takahashi, N.M. Dung, K. Matsumoto, I. Shimoyama, Differential pressure sensor using a piezoresistive cantilever, J. Micromech. Microeng. 22 (2012), 055015.
[120] A.K. Dhonkal, V. Agarwal, K. Sengar, Sensitivity of the MEMS based piezoresistive wind speed sensor with comparative study of different shapes of paddles, Int. Res. J. Eng. Sci. Technol. 4 (2017) 1693–1697.
[121] B. Tian, H. Li, N. Yang, H. Liu, Y. Zhao, A MEMS-based flow sensor with membrane cantilever beam array structure, 2017 IEEE 12th International Conference on Nano/Micro Engineered and Molecular Systems (NEMS) (2017) 185–189.
[122] H. Takahashi, A. Nakai, I. Shimoyama, Waterproof airflow sensor for seabird bio-logging using a highly sensitive differential pressure sensor and nano-hole array, Sens. Actuators A Phys. 281 (2018) 243–249.
[123] Y. Su, A.G.R. Evans, A. Brunnschweiler, Micromachined silicon cantilever paddles with piezoresistive readout for flow sensing, J. Micromech. Microeng. 6 (1996) 69–72.
[124] J. Zou, J. Chen, C. Liu, J.E. Schutt-Ainé, Plastic deformation magnetic assembly (PDMA) of out-of-plane microstructures: technology and application, J. Microelectromech. Syst. 10 (2001) 302–309.
[125] M.R. Maschmann, G.J. Ehlert, B.T. Dickinson, D.M. Phillips, C.W. Ray, G.W. Reich, et al., Bioinspired carbon nanotube fuzzy fiber hair sensor for air-flow detection, Adv. Mater. 26 (2014) 3230–3234.
[126] H. Devaraj, J. Travas-Sejdic, R. Sharma, N. Aydemir, D. Williams, E. Haemmerle, et al., Bio-inspired flow sensor from printed PEDOT:PSS micro-hairs, Bioinspir. Biomim. 10 (2015).
[127] X. Sun, J.L. Tao, J.L. Li, Q.L. Dai, X. Yu, Aeroelastic-aerodynamic analysis and bio-inspired flow sensor design for boundary layer velocity profiles of wind turbine blades with active external flaps, Smart Struct. Syst. 20 (2017) 311–328.
[128] Y.H. Wang, C.P. Chen, C.M. Chang, C.P. Lin, C.H. Lin, L.M. Fu, et al., MEMS-based gas flow sensors, Microfluid. Nanofluidics 6 (2009) 333–346.
[129] H. Bleckmann, R. Zelick, Lateral line system of fish, Integr. Zool. 4 (2009) 13–25.
[130] J.F. Webb, J.C. Montgomery, J. Mogdans, Bioacoustics and the Lateral Line System of Fishes, Fish Bioacoustics, Springer, New York, NY, 2008, pp. 145–182.
[131] Y. Yang, N. Chen, C. Tucker, J. Engel, S. Pandya, C. Liu, From artificial hair cell sensor to artificial lateral line system: development and application, 2007 IEEE 20th International Conference on Micro Electro Mechanical Systems (MEMS) (2007) 577–580.
[132] G. Zhou, Y. Zhao, F. Guo, W. Xu, A smart high accuracy silicon piezoresistive pressure sensor temperature compensation system, Sensors 14 (2014) 12174–12190.
[133] S. Sushmita, S.M. Hiremath, Kulkarni, Modelling and analysis of polymer diaphragms for micro sensing and actuation, in: AIP Conference Proceedings, AIP Publishing, 2019, pp. 020004.
[134] N. Chen, C. Tucker, J.M. Engel, Y. Yang, S. Pandya, C. Liu, Design and characterization of artificial haircell sensor for flow sensing with ultrahigh velocity and angular sensitivity, J. Microelectromech. Syst. 16 (2007) 999–1014.
[135] H. Hu, C. Liu, N. Chen, A robust tactile shear stress sensor derived from a bio-inspired artificial haircell sensor, in: Proceedings of IEEE Sensors, 2008, pp. 1517–1519.
[136] A.G.P. Kottapalli, M. Bora, E. Kanhere, M. Asadnia, J. Miao, M.S. Triantafyllou, Cupula-inspired hyaluronic acid-based hydrogel encapsulation to form biomimetic MEMS flow sensors, Sensors 17 (2017) 1728.
[137] S. Peleshanko, M.D. Julian, M. Ornatska, M.E. McConney, M.C. LeMieux, N. Chen, et al., Hydrogel-encapsulated microfabricated haircells mimicking fish cupula neuromast, Adv. Mater. 19 (2007) 2903–2909.
[138] K.D. Anderson, D. Lu, M.E. McConney, T. Han, D.H. Reneker, V.V. Tsukruk, Hydrogel microstructures combined with electrospun fibers and photopatterning for shape and modulus control, Polymer 49 (2008) 5284–5293.
[139] A.G.P. Kottapalli, C.W. Tan, M. Olfatnia, J.M. Miao, G. Barbastathis, M. Triantafyllou, A liquid crystal polymer membrane MEMS sensor for flow rate and flow direction sensing applications, J. Micromech. Microeng. 21 (2011).
[140] J. Chen, J. Engel, C. Liu, Development of polymer-based artificial haircell using surface micromachining and 3D assembly, 12th International Conference on Solid-State Sensors, Actuators and Microsystems Digest of Technical Papers (2003) 1035–1038.
[141] J.M. Engel, J. Chen, C. Liu, D. Bullen, Polyurethane rubber all-polymer artificial hair cell sensor, J. Microelectromech. Syst. 15 (2006) 729–736.
[142] J.M. Engel, J. Chen, D. Bullen, C. Liu, Polyurethane rubber as a MEMS material: characterization and demonstration of an all-polymer two-axis artificial hair cell flow sensor, Proceedings of the IEEE International Conference on Micro Electro Mechanical Systems (MEMS) (2005) 279–282.
[143] C. Tucker, N. Chen, J. Engel, Y. Yang, S. Pandya, C. Liu, High-sensitivity bi-directional flow sensor based on biological inspiration of animal haircell sensors, Proceedings of IEEE Sensors (2006) 1440–1442.
[144] Z. Fan, J. Chen, J. Zou, D. Bullen, C. Liu, F. Delcomyn, Design and fabrication of artificial lateral line flow sensors, J. Micromech. Microeng. 12 (2002) 655–661.
[145] A.P. Kottapalli, M. Asadnia, J. Miao, M. Triantafyllou, Electrospun nanofibrils encapsulated in hydrogel cupula for biomimetic MEMS flow sensor development, 2013 IEEE 26th International Conference on Micro Electro Mechanical Systems (MEMS) (2013) 25–28.
[146] A.G.P. Kottapalli, C.W. Tan, M. Olfatnia, J.M. Miao, G. Barbastathis, M. Triantafyllou, A liquid crystal polymer membrane MEMS sensor for flow rate and flow direction sensing applications, J. Micromech. Microeng. 21 (2011), 085006.
[147] A.G.P. Kottapalli, M. Asadnia, J.M. Miao, G. Barbastathis, M.S. Triantafyllou, A flexible liquid crystal polymer MEMS pressure sensor array for fish-like underwater sensing, Smart Mater. Struct. 21 (2012).
[148] A.G.P. Kottapalli, M. Asadnia, J. Miao, M. Triantafyllou, Soft polymer membrane micro-sensor arrays inspired by the mechanosensory lateral line on the blind cavefish, J. Intell. Mater. Syst. Struct. 26 (2015) 38–46.
[149] A.G.P. Kottapalli, M. Asadnia, J. Miao, M. Triantafyllou, Touch at a distance sensing: lateral-line inspired MEMS flow sensors, Bioinspir. Biomim. 9 (2014), 046011.
[150] Z. Shen, A.G.P. Kottapalli, V. Subramaniam, M. Asadnia, J. Miao, M. Triantafyllou, Biomimetic flow sensors for biomedical flow sensing in intravenous tubes, 2016 IEEE SENSORS (2016) 1–3.
[151] H. Herzog, A. Klein, H. Bleckmann, P. Holik, S. Schmitz, G. Siebke, et al., μ-biomimetic flow-sensors—introducing light-guiding PDMS structures into MEMS, Bioinspir. Biomim. 10 (2015), 036001.
[152] V.I. Fernandez, S.M. Hou, F.S. Hover, J.H. Lang, M.S. Triantafyllou, Lateral-line Inspired MEMS-array Pressure Sensing for Passive Underwater Navigation, MIT Sea Grant Technical Reports, Massachusetts Institute of Technology, 2007.
[153] M. Nawi, A. Manaf, M. Arshad, O. Sidek, Development of microfluidic based multidirectional flow sensor inspired from artificial cupula, Microsyst. Technol. 21 (2015) 1513–1521.
[154] R. Mathew, A.R. Sankar, A review on surface stress-based miniaturized piezoresistive SU-8 polymeric cantilever sensors, Nano Micro Lett. 10 (2018).
[155] R. Hagihghi, A. Razmjou, Y. Orooji, M.E. Warkiani, M. Asadnia, A miniaturized piezoresistive flow sensor for real-time monitoring of intravenous infusion, J. Biomed. Mater. Res. Part B Appl. Biomater. (2019), 0.
[156] S. Peleshanko, M.D. Julian, M. Ornatska, M.E. McConney, M.C. LeMieux, N. Chen, et al., Hydrogel-encapsulated microfabricated haircells mimicking fish cupula neuromast, Adv. Mater. 19 (2007) 2903-+.
[157] N.N. Chen, C. Tucker, J.M. Engel, Y.C. Yang, S. Pandya, C. Liu, Design and characterization of artificial haircell sensor for flow sensing with ultrahigh velocity and angular sensitivity, J. Microelectromech. Syst. 16 (2007) 999–1014.
[158] D. Celentano, D. Wimmer, L. Colabella, A.P. Cisilino, Viscoelastic mechanical characterization of a short-fiber reinforced polyethylene tube: experiments and modelling, Int. J. Press. Vessel. Pip. 134 (2015) 82–91.
[159] S. Keller, G. Blagoi, M. Lillemose, D. Haefliger, A. Boisen, Processing of thin SU-8 films, J. Micromechanics Microengineering 18 (2008), 125020.
[160] C. Martin, A. Llobera, G. Villanueva, A. Voigt, G. Gruetzner, J. Brugger, et al., Stress and aging minimization in photoplastic AFM probes, Microelectron. Eng. 86 (2009) 1226–1229.
[161] M. Asadnia, A.G.P. Kottapalli, J. Miao, A.B. Randles, A. Sabbagh, P. Kropelnicki, et al., High temperature characterization of PZT(0.52/0.48) thin-film pressure sensors, J. Micromech. Microeng. 24 (2014), 015017.
[162] M. Asadnia, A. Kottapalli, J. Miao, A. Randles, A. Sabbagh, P. Kropelnicki, et al., High temperature characterization of PZT (0.52/0.48) thin-film pressure sensors, J. Micromech. Microeng. 24 (2013), 015017.
[163] B.C. Zhou, R. Li, J. Cai, J. Xu, Z.H. Zhao, J.Z. Pei, Grain size effect on electric properties of novel BaTiO3/PVDF composite piezoelectric ceramics, Mater. Res. Express 5 (2018).
[164] H. Khan, A. Razmjou, M. Ebrahimi Warkiani, A. Kottapalli, M. Asadnia, Sensitive and flexible polymeric strain sensor for accurate human motion monitoring, Sensors 18 (2018) 418.
[165] D. Sengupta, A.G.P. Kottapalli, S.H. Chen, J.M. Miao, C.Y. Kwok, M.S. Triantafyllou, et al., Characterization of single polyvinylidene fluoride (PVDF) nanofiber for flow sensing applications, AIP Adv. 7 (2017).
[166] S.R. Anton, H.A. Sodano, A review of power harvesting using piezoelectric materials (2003–2006), Smart Mater. Struct. 16 (2007) R1–R21.
[167] J. Chang, M. Domnner, C. Chang, L. Lin, Piezoelectric nanofibers for energy scavenging applications, Nano Energy 1 (2012) 356–371.
[168] M. Asadnia, S.M.M. Ehteshami, S.H. Chan, M.E. Warkiani, Development of a fiber-based membraneless hydrogen peroxide fuel cell, RSC Adv. 7 (2017) 40755–40760.
[169] Y.-F. Goh, I. Shakir, R. Hussain, Electrospun fibers for tissue engineering, drug delivery, and wound dressing, J. Mater. Sci. 48 (2013) 3027–3054.
[170] D. Mandal, S. Yoon, K.J. Kim, Origin of Piezoelectricity in an electrospun poly(vinylidene fluoride-trifluoroethylene) nanofiber web-based nanogenerator and nano-pressure sensor, Macromol. Rapid Commun. 32 (2011) 831–837.

[171] W.-Y. Chang, C.-H. Chu, Y.-C. Lin, A Flexible piezoelectric sensor for microfluidic applications using polyvinylidene fluoride, IEEE Sens. J. 8 (2008) 495–500.
[172] W. Jung, C. Li, D.-S. Kim, C.H. Ahn, A sensing tube with an integrated piezoelectric flow sensor for liver transplantation, 2009 Annual International Conference of the IEEE Engineering in Medicine and Biology SoCiety (2009) 4469–4472.
[173] T. Sharma, S.-S. Je, B. Gill, J.X. Zhang, Patterning piezoelectric thin film PVDF–TrFE based pressure sensor for catheter application, Sens. Actuators A Phys. 177 (2012) 87–92.
[174] M. Asadnia, A.G.P. Kottapalli, K.D. Karavitaki, M.E. Warkiani, J. Miao, D.P. Corey, et al., From biological cilia to artificial flow sensors: biomimetic soft polymer nanosensors with high sensing performance, Sci. Rep. 6 (2016) 32955.
[175] A.G.P. Kottapalli, M. Asadnia, K.D. Karavitaki, M.E. Warkiani, J. Miao, D.P. Corey, et al., Engineering biomimetic hair bundle sensors for underwater sensing applications, in: AIP Conference Proceedings, AIP Publishing, 2018, pp. 160003.
[176] M. Olfatnia, Z. Shen, J.M. Miao, L.S. Ong, T. Xu, M. Ebrahimi, Medium damping influences on the resonant frequency and quality factor of piezoelectric circular microdiaphragm sensors, J. Micromech. Microeng. 21 (2011).
[177] M. Olfatnia, T. Xu, J.M. Miao, L.S. Ong, X.M. Jing, L. Norford, Piezoelectric circular microdiaphragm based pressure sensors, Sensors and Actuators a-Physical 163 (2010) 32–36.
[178] Z.H. Wang, X.X. Zhang, X.B. Wang, W.S. Yue, J.Q. Li, J.M. Miao, et al., Giant flexoelectric polarization in a micromachined ferroelectric diaphragm, Adv. Funct. Mater. 23 (2013) 124–132.
[179] B. Jaffe, Piezoelectric ceramics, 2019.
[180] T. Iijima, N. Kochi, S. Okamura, Impedance response of lead zirconate titanate thick film structures on silicon substrates for a high frequency ultrasonic transducer, J. Ceram. Soc. Jpn. 121 (2013) 670–674.
[181] S.-C. Lin, W.-J. Wu, Fabrication of PZT MEMS energy harvester based on silicon and stainless-steel substrates utilizing an aerosol deposition method, J. Micromech. Microeng. 23 (2013).
[182] A.J. Pickwell, R.A. Dorey, D. Mba, Development of a thick film PZT foil sensor for use in structural health monitoring applications, IEEE Trans. Ultrason. Ferroelectr. Freq. Control 60 (2013) 373–379.
[183] W. Zhang, D. Xu, J. Ouyang, Converse longitudinal piezoelectric response of a ferroelectric thick film elastically coupled with a supporting substrate or underlayer, J. Phys. D Appl. Phys. 46 (2013).
[184] D. Balma, A. Mazzalai, N. Chidambaram, C.S. Sandu, A. Neels, A. Dommann, et al., High piezoelectric longitudinal coefficients in sol-gel PZT thin film multilayers, J. Am. Ceram. Soc. 97 (2014) 2069–2075.
[185] S.S. Bedair, J.S. Pulskamp, R.G. Polcawich, B. Morgan, J.L. Martin, B. Power, Thin-film piezoelectric-on-Silicon resonant transformers, J. Microelectromech. Syst. 22 (2013) 1383–1394.
[186] X. Chen, C. Qiu, H. Liu, Y. Dou, S. Gao, Research of complex PZT film Base on shear mode energy harvesting, in: W.P. Sung, R. Chen (Eds.), Biotechnology, Chemical and Materials Engineering Iii, Pts 1 and 2, 2014, pp. 363–369.
[187] T. Naono, T. Fujii, M. Esashi, S. Tanaka, A large-scan-angle piezoelectric MEMS optical scanner actuated by a Nb-doped PZT thin film, J. Micromech. Microeng. 24 (2014).
[188] Y. Tomimatsu, K. Kuwana, T. Kobayashi, T. Itoh, R. Maeda, A piezoelectric flow sensor for wake-up switch of wireless sensor network node, 2012 Second Workshop on Design, Control and Software Implementation for Distributed MEMS (2012) 53–57.
[189] A.G.P. Kottapalli, M. Asadnia, H. Hans, J.M. Miao, M.S. Triantafyllou, Harbor seal inspired MEMS artificial micro-whisker sensor, 2014 IEEE 27th International Conference on Micro Electro Mechanical Systems (MEMS) (2014) 741–744.
[190] M. Bora, A.G.P. Kottapalli, J.M. Miao, M.S. Triantafyllou, Fish-inspired self-powered microelectromechanical flow sensor with biomimetic hydrogel cupula, APL Mater. 5 (2017), 104902.
[191] A. Kuoni, R. Holzherr, B. Boillat, N.F. De Rooij, Polyimide membrane with ZnO piezoelectric thin film pressure transducers as a differential pressure liquid flow sensor, J. Micromech. Microeng. 13 (2003) S103–S107.
[192] J. Tao, X. Yu, J. Berilla, Micropillar sensing element for bio-inspired flow sensors, 8th International Workshop on Structural Health Monitoring 2011: Condition-Based Maintenance and Intelligent Structures (2011).
[193] X. Guo, B. Yang, Q. Wang, C. Lu, D. Hu, Design and characterization of a novel bio-inspired hair flow sensor based on resonant sensing, J. Phys. Conf. Ser. (2018) 012005, IOP Publishing.
[194] C. Steinem, A. Janshoff, Piezoelectric Sensors, Springer, Verlag Berlin Heidelberg, 2007.
[195] J.M. Herbert, Ferroelectric Transducers and Sensors, 1982, pp. 3.
[196] S.D. Nguyen, I. Paprotny, P.K. Wright, R.M. White, MEMS capacitive flow sensor for natural gas pipelines, Sens. Actuators A Phys. 231 (2015) 28–34.
[197] O. Berberig, K. Nottmeyer, J. Mizuno, Y. Kanai, T. Kobayashi, The Prandtl micro flow sensor (PMFS): a novel silicon diaphragm capacitive sensor for flow-velocity measurement, Sens. Actuators A Phys. 66 (1998) 93–98.
[198] J. Jaesung, S.T. Wereley, A capacitive micro gas flow sensor based on slip flow, in: 17th IEEE International Conference on Micro Electro Mechanical Systems Maastricht MEMS 2004 Technical Digest, 2004, pp. 540–543.
[199] S.F. Mousavi, S.H. Hashemabadi, H. Azizi Moghaddam, Design, simulation, fabrication and testing of ultrasonic gas flowmeter transducer (sensor), Sens. Rev. 39 (2019) 277–287.
[200] D. Han, S. Kim, S. Park, Two-dimensional ultrasonic anemometer using the directivity angle of an ultrasonic sensor, Microelectronics J. 39 (2008) 1195–1199.
[201] T.V.P. Schut, D. Alveringh, W. Sparreboom, J. Groenesteijn, R.J. Wiegerink, J.C. Lotters, Fully integrated mass flow, pressure, density and viscosity sensor for both liquids and gases, in: 2018 IEEE Micro Electro Mechanical Systems (MEMS), 2018, pp. 218–221.
[202] J. Haneveld, T.S.J. Lammerink, M.Jd. Boer, R.J. Wiegerink, Micro coriolis mass flow sensor with integrated capacitive readout, in: 2009 IEEE 22nd International Conference on Micro Electro Mechanical Systems, 2009, pp. 463–466.
[203] R. Smith, D.R. Sparks, D. Riley, N. Najafi, A MEMS-based coriolis mass flow sensor for industrial applications, IEEE Trans. Ind. Electron. 56 (2009) 1066–1071.
[204] S.I. Abdullahi, N.A. Malik, M.H. Habaebi, A.B. Salami, Miniaturized turbine flow sensor: design and simulation, in: 2018 7th International Conference on Computer and Communication Engineering (ICCCE), 2018, pp. 38–43.
[205] P. Bruschi, M. Dei, M. Piotto, An offset compensation method with low residual drift for integrated thermal flow sensors, IEEE Sens. J. 11 (2011) 1162–1168.
[206] M. Piotto, M. Dei, F. Butti, G. Pennelli, P. Bruschi, Smart flow sensor with on-chip CMOS interface performing offset and pressure effect compensation, IEEE Sens. J. 12 (2012) 3309–3317.
[207] M. Mansoor, I. Haneef, S. Akhtar, M.A. Rafiq, A. De Luca, S.Z. Ali, et al., An SOI CMOS-Based multi-sensor MEMS chip for fluidic applications, Sensors 16 (2016).

Biographies

Fatemeh Ejeian is a Ph.D. candidate in Nano-biotechnology at the University of Isfahan-Iran and Macquarie University. She received her M.Sc. degree in Cellular and molecular Biology from University of Tehran, Iran. Her research interests include regenerative medicine, biomimetic cell culture substrates, and bio-inspired MEMS/NEMS sensors. She is currently working on designing particular geometrical patterned substrates for regulation of MSCs behavior.

Shohreh Azadi is a PhD candidate at AmirKabir University-Iran and School of Engineering Macquarie University. She received both her Bachelor and Master degree in Biomedical Engineering at Tehran Polytechnic. During her study, she joined Pasteur Institute and Stem cell research center in Tehran/Iran and worked on cancer cell mechanics. Her current research involves mechanical behavior of cancer cells and their migration and invasion ability using 3D microfluidic systems and fellow sensory systems.

Amir Razmjou received his PhD from UNSW 2012, Australia and has been spending more than a decade on teaching, research and development. He has accrued multidisciplinary skills to develop innovative technologies for biomedical and environmental applications. His surface architecturing skills using functional nanostructured materials alongside biofunctionalization have helped him to develop innovative nano structured membranes for desalination and water treatment, drug delivery systems, and biosensors.

Yasin Orooji is an associate professor College of Materials Science and Engineering, Nanjing Forestry University. His field of interests are Biofouling mitigation and porous materials.

Ajay Kottapalli received his M.Sc. degree in Physics with specialization in Photonics in 2007. Later on, he obtained an M.Tech. degree in Solid State Technology from the Indian Institute of Technology, Madras, (IIT-M) India. He worked as an Applications Engineer in KLA Tencor Pvt Ltd and is trained in semiconductor wafer defect inspection in silicon valley California. In 2010, he started his Ph.D. studies at Nanyang Technological University (NTU) Singapore under the supervision of Prof. Miao Jianmin and Prof. Michael Triantafyllou. During his Ph.D., His Ph.D. thesis is on the development of biomimetic ultra sensitive NEMS flow sensors inspired by the ingenuity of the neuromast sensors in the blind cavefish. His research interests include biomimetics, bio-inspired MEMS/NEMS sensors, soft-polymer sensors, biomaterials, nature-inspired sensors, piezoelectric actuators, etc.

Majid E. Warkiani is a Senior Lecturer in the School of Biomedical Engineering, UTS, Sydney, Australia. He received his Ph.D. in Mechanical Engineering from Nanyang Technological University (NTU) and undertook postdoctoral training at Massachusetts Institute of Technology (SMART centre). He is also a member of Institute for Biomedical Materials & Devices (IBMD) and Center for Health Technologies (CHT) at UTS. Dr Warkiani's current research activities focus on three key areas of (i) Microfluidics involving the design and development of novel microfluidic systems for particle and cell sorting (e.g., circulating tumor cells, fetal cells & stem cells) for diagnostic and therapeutic applications, (ii) Bio-MEMS involving the fabrication and characterization of novel 3D lab-on-a-chip systems to model physiological functions of tissues and organs, and (iii) 3D Printing involving the design and development of novel miniaturized systems (e.g., micromixers, micro-cyclones) for basic and applied research.

Mohsen Asadnia Dr. Mohsen Asadnia is a senior lecturer in Mechatronics-biomechanics and an ARC DECRA Fellow at Macquarie University. Prior to this, he was a research associate at the University of Western Australia, and before this a postdoctoral research fellow at the Massachusetts Institute of Technology (Singapore-MIT Alliance for Research and Technology Centre). He received his PhD degree in Mechanical Engineering from Nanyang Technological University-Singapore. He has received over $2m research funding from the Australian Research Council (DECRA and LIEF), the Australian Academy of Science (regional collaboration programme) and the National Research Foundation Singapore. He is a pioneer in the use of piezoelectric materials in MEMS chemical and physical sensors for biomedical applications, and his research group continues to break new ground in this cutting-edge area of inter-disciplinary chemistry, auditory haircells and microfluidics.